Clustering, lensing, and ISW/Rees-Sciama from the DEMNUni neutrino simulations

Carmelita Carbone

INAF - Astronomical Observatory of Brera (Milan)

This project has received funding from the European Union's Seventh Framework Programme for research, technological development and demonstration under grant agreement no 291521

Nonlinear evolution of the LSS of the Universe: theory meets expectations May 26th, 2016, IAP, Paris

Massive neutrino effects in the linear regime

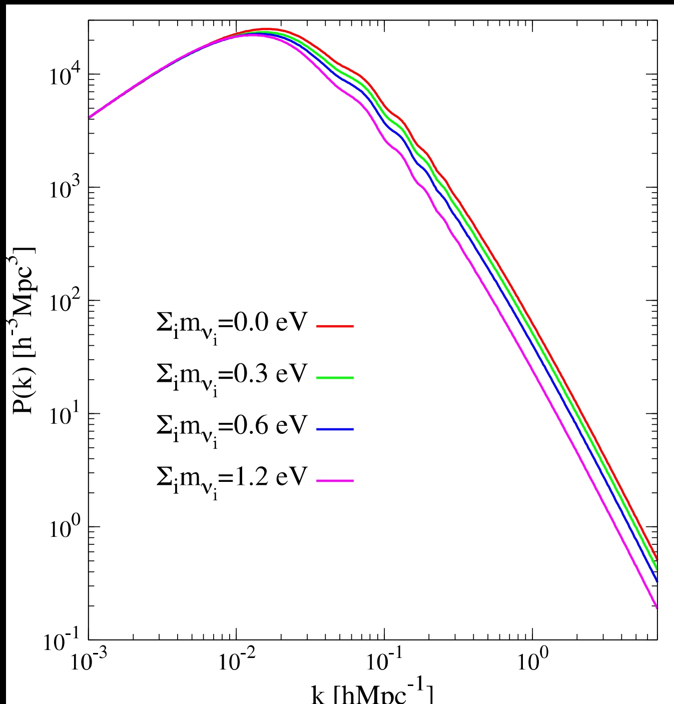

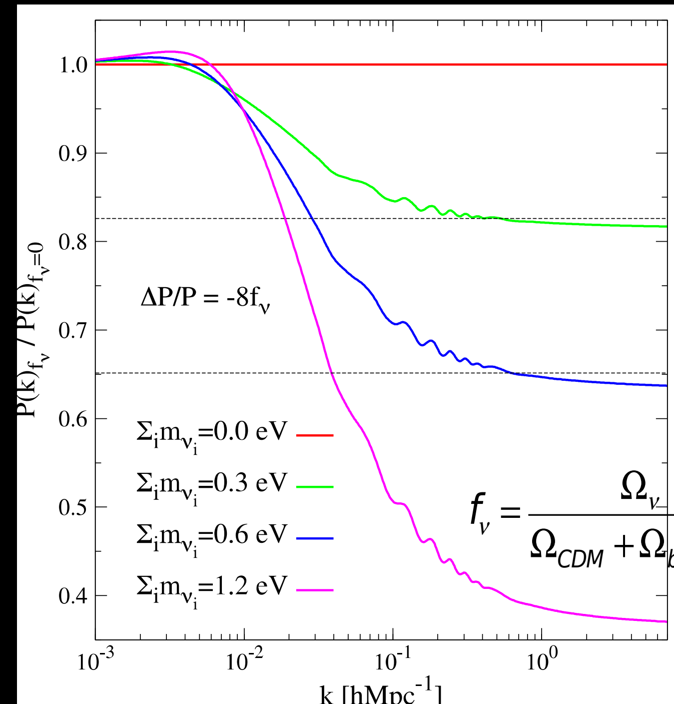

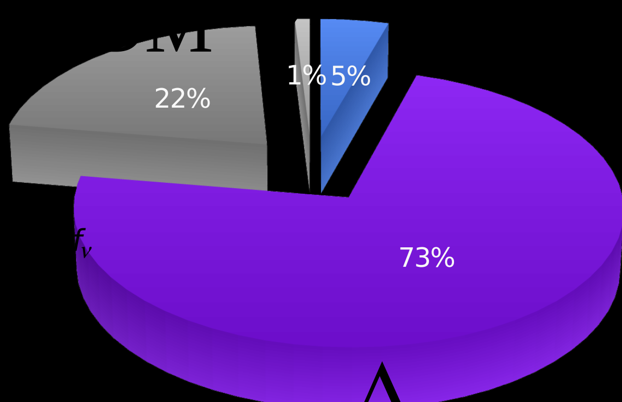

1. **Modification of the Matter-Radiation equality time**
2. **Slow down the growth of matter perturbations**

Lesgourgues & Pastor, Physics Reports, 429, 6, 2006

Spectro-Euclid forecasts

Table 5: $\sigma(M_\nu)$ and $\sigma(N_{\rm eff})$ marginalised errors from LSS+CMB

	General cosmology					
fiducial→	M_ν=0.3 eV[a]	M_ν=0.2 eV[a]	M_ν=0.125 eV[b]	M_ν=0.125 eV[c]	M_ν=0.05 eV[b]	$N_{\rm eff}$=3.04[d]
slitless+BOSS+Planck	0.035	0.043	0.031	0.044	0.053	0.086
	ΛCDM cosmology					
slitless+BOSS+Planck	0.017	0.019	0.017	0.021	0.021	0.023

[a] for degenerate spectrum: $m_1 \approx m_2 \approx m_3$; [b] for normal hierarchy: $m_3 \neq 0$, $m_1 \approx m_2 \approx 0$
[c] for inverted hierarchy: $m_1 \approx m_2$, $m_3 \approx 0$; [d] fiducial cosmology with massless neutrinos

Only 3 active neutrinos for M_ν errors

CC et al. 2011

If M_ν is > 0.1 eV, spectroscopic Euclid will be able to determine the neutrino mass scale independently of the model cosmology assumed. If M_ν is < 0.1 eV, the sum of neutrino masses, and in particular the minimum neutrino mass required by neutrino oscillations, can be measured in the context of a LCDM model. DE FoM decreases by a factor 2-3 wrt the massless case. Important to include NL info.

Effects in the non-linear regime

<u>Why?</u>

- Important on small scales
- Important at low redshift
- Lots of modes in the middle—non-linear regime

<u>How?</u>

- Semi-analytic methods
  N-1-body, Ringwald & Wong, 2004
  (see also Singh & Ma, 2003)
- Perturbation theory
  Blas, Garny, Konstandin, Lesgourgues, 2014
- N-body simulations
  Particle/Grid based/Boltzmann

Simulating neutrinos as particles

Add neutrinos as an extra dark matter particle species
with large thermal velocity given by the FD distribution

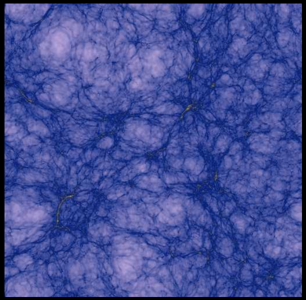

CDM

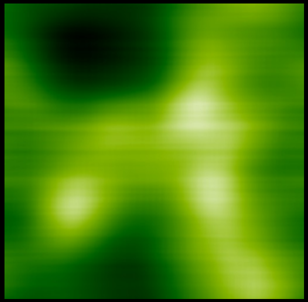

Neutrinos

(Viel etal 2010)

Works best for large neutrino masses
Simple, easy to implement

N-body simulations with neutrino particles

	CDM	CDM + ν
Power spectrum	$P_m(k)$ 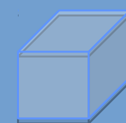	$P_{cb}(k)$ $P_\nu(k)$ 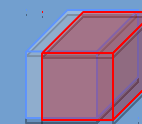
Growth factor	Scale independent	Scale dependent
Growth rate	Scale independent	Scale dependent
Velocities	Peculiar	Peculiar Peculiar + thermal

Effects on matter power spectrum

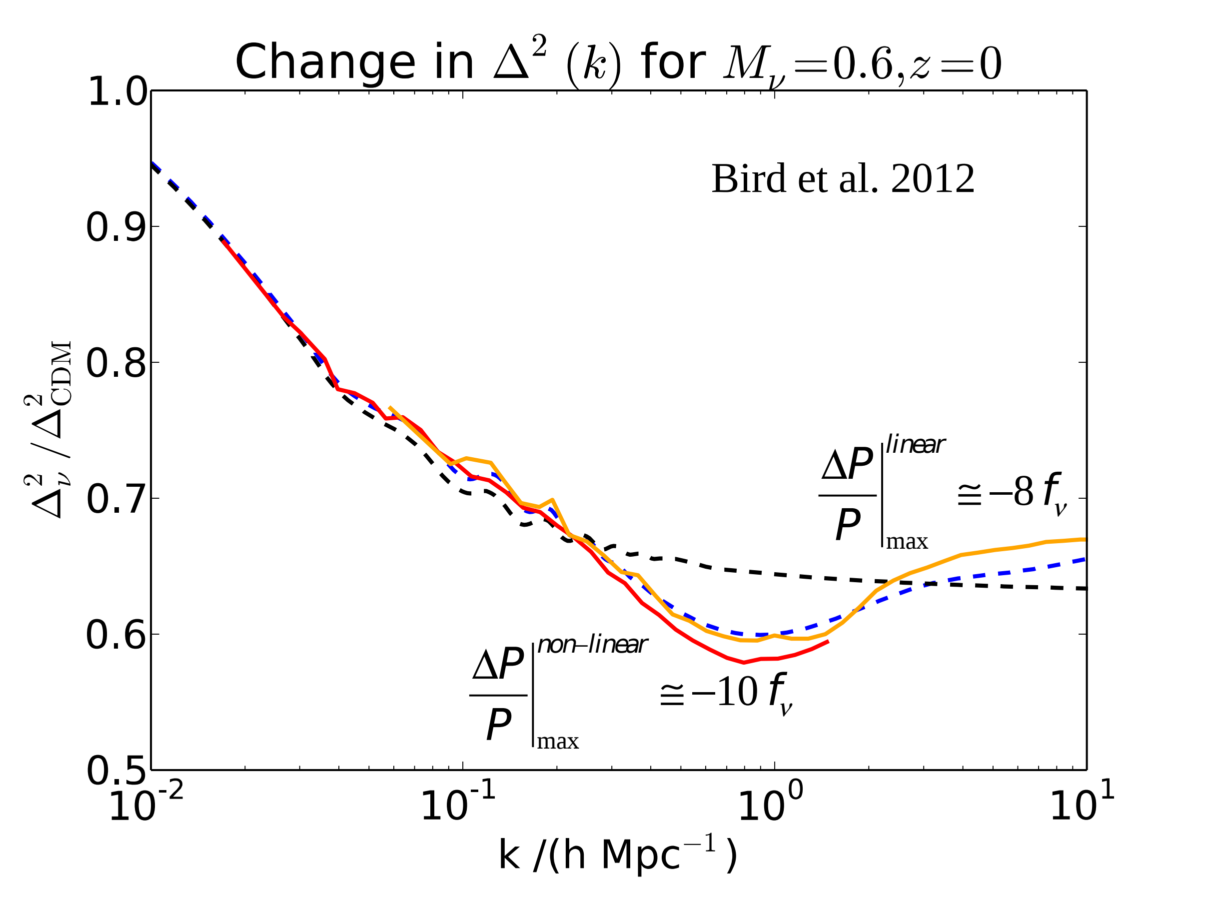

512 Mpc/h

150 Mpc/h

Fitting formula

Linear prediction

Brandbyge, Hannestad, Haugbolle, Thomsen, 2008
Viel, Haehnelt, Springel, 2010
Bird, Viel, Haehnelt, 2012
Wagner, Verde, Jimenez, 2012
Ali-Haïmoud&Bird, 2012
Agarwal, Feldman, 2011
Massara, FVN, Viel, 2014
Rossi, Palanque-Delabrouille, Borde, Viel, Yeche, Bolton, Rich, Le Goff, 2014
Upadhye, Biswas, Pope, Heitmann, Habib, Finkel, Frontiere, 2014
Inman, Emberson, Pen, Farchi, Yu, Harnois-Deraps, 2015
CC et al 2016

DEMNUni simulations (PI Carbone)

- **$(5+8)\times10^{6}$ cpu-hours on Tier-0 BGQ/FERMI at CINECA**
- **4 mixed dark matter cosmological simulations for CMB and LSS analysis in the presence of massive neutrinos and 10 more with M_ν-w_0-w_a by the end of 2016**
- **Planck cosmology M_ν=0, 0.17, 0.3, 0.53 eV**
- **Gadget-3 with ν-particle component (Viel et al. 2010)**
- **box-side size: 2 Gpc/h**
- **particle number: 2 x 2048^3 (CDM+ν);**
- **PMGRID: 4096 (2Np)**
- **CDM mass: 8 x 10^{10} $M_{\odot}$/h (neutrino particle mass depends on M_ν, 1% at k=1)**
- **softening length: 20 kpc/h**
- **starting redshift: z =99**

$$k_{\rm nr} = 0.018(m_\nu/1{\rm eV})^{1/2}\Omega_m^{1/2}h/{\rm Mpc}$$

Simulation outputs

- 90 TB/sim of data
- 62 temporary snapshots per simulation: ~0.54 TB/snap (CDM+ ν)
- 62 halo-catalogs
- 62 sub-halo catalogs
- Matter power-spectra and correlation functions for all the 62 snapshots
- 62 temporary gravitational potential grids of size 4096^3 (for CMB weak-lensing)
- 62 temporary grids of size 4096^3 for the derivative of the gravitational potential (for ISW/Rees-Sciama)

Castorina, CC et al. 2015

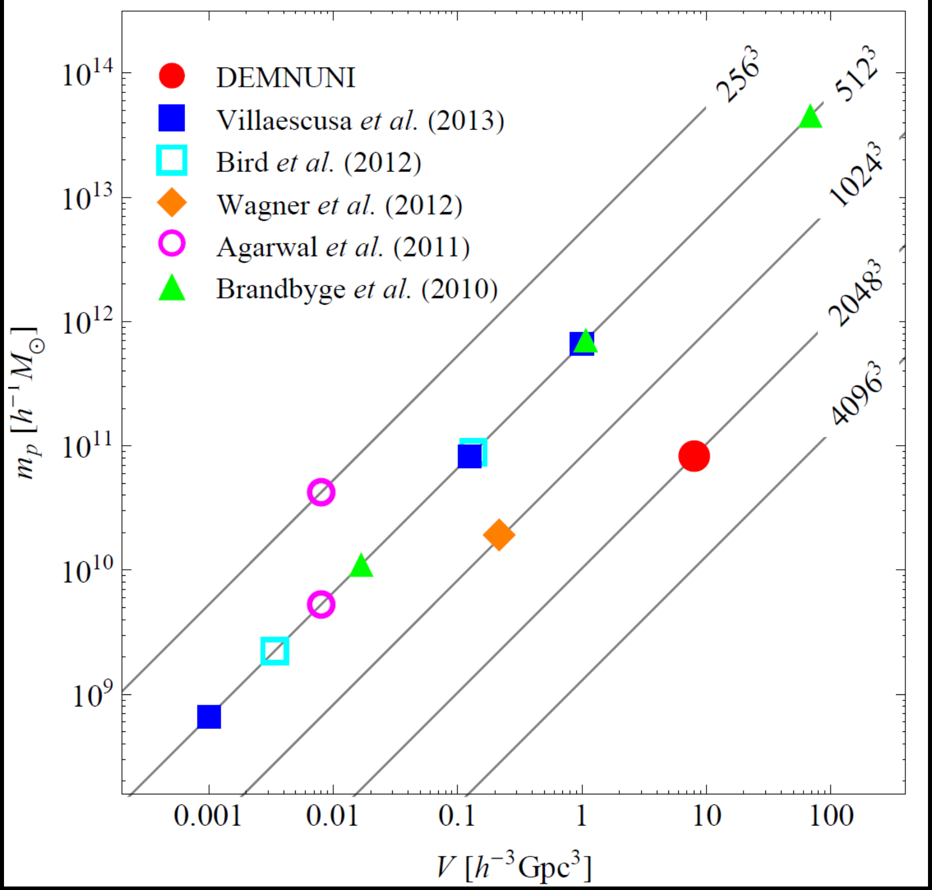

Comparison between the DEMNUni runs and previous, recent simulations of massive neutrino cosmologies in terms of cold dark matter mass resolution and volume

DEMNUni matter power spectra for M_ν=0.3 eV

CC et al. 2016

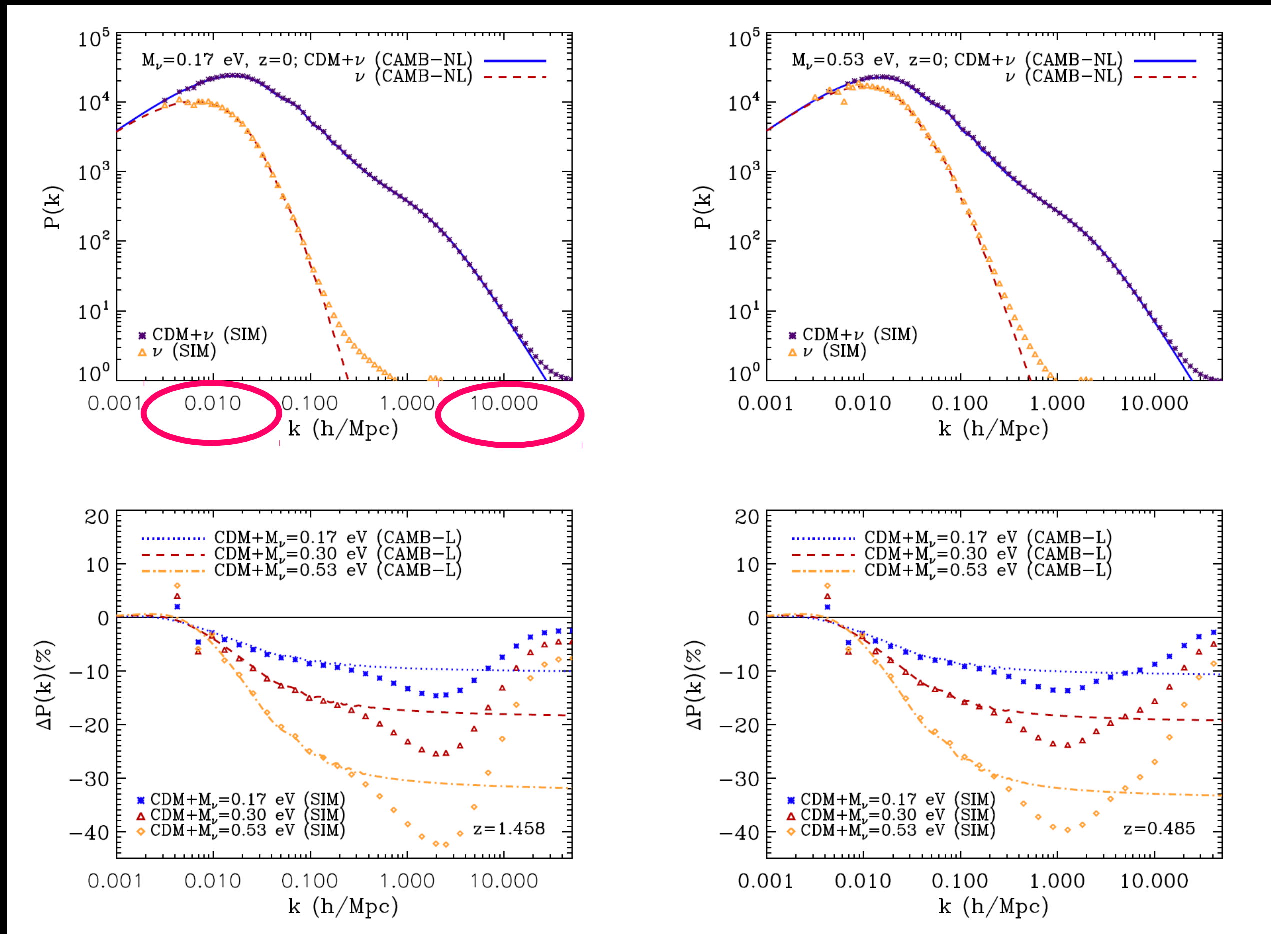

The large volume and mass resolution of the DEMNUni simulations allow to test different probes, and their combinations, in massive neutrino cosmologies, at the level of accuracy required by current and future galaxy surveys.

$$k_{\rm fs}(z) = 0.82 H(z)/H_0/(1+z)^2 (m_\nu/1{\rm eV}) \; h{\rm Mpc}^{-1}$$

CDM- and ν-halos from the DEMNUni simulations

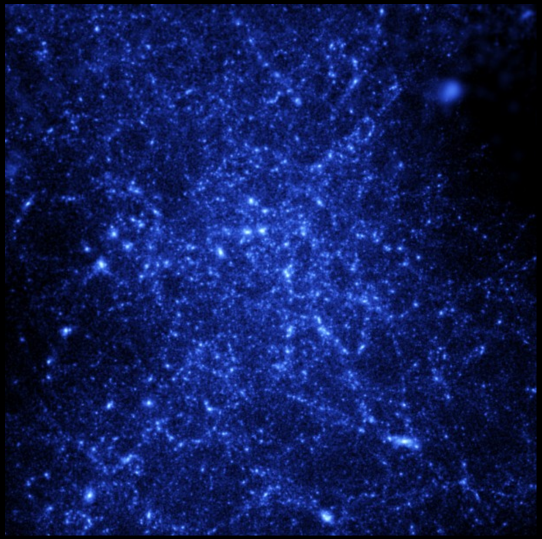

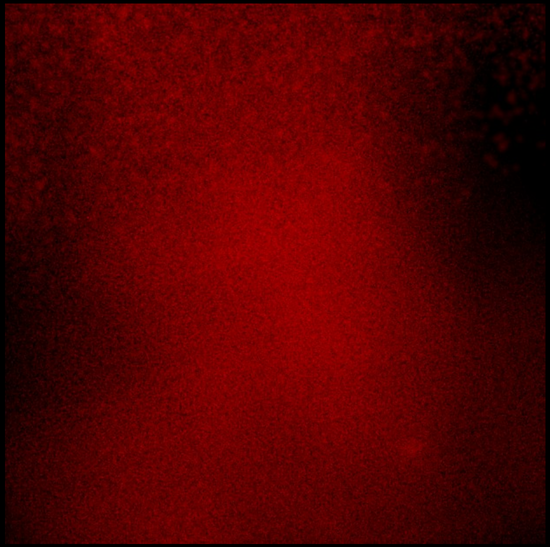

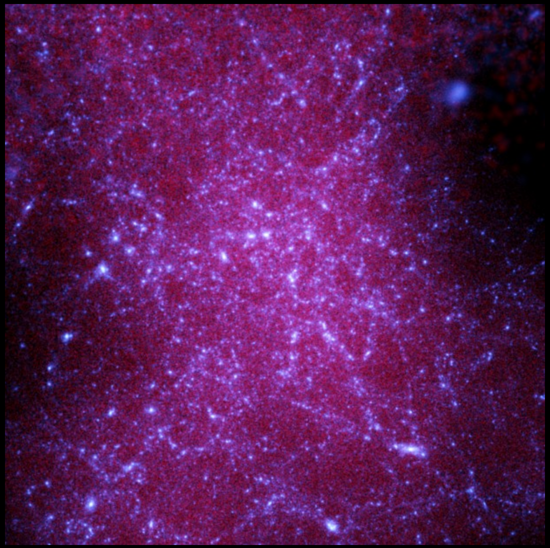

CDM density

ν density

CDM+ν density

CDM/ν clustering in high resolution simulations
(about 2400 times smaller than DEMNUni)

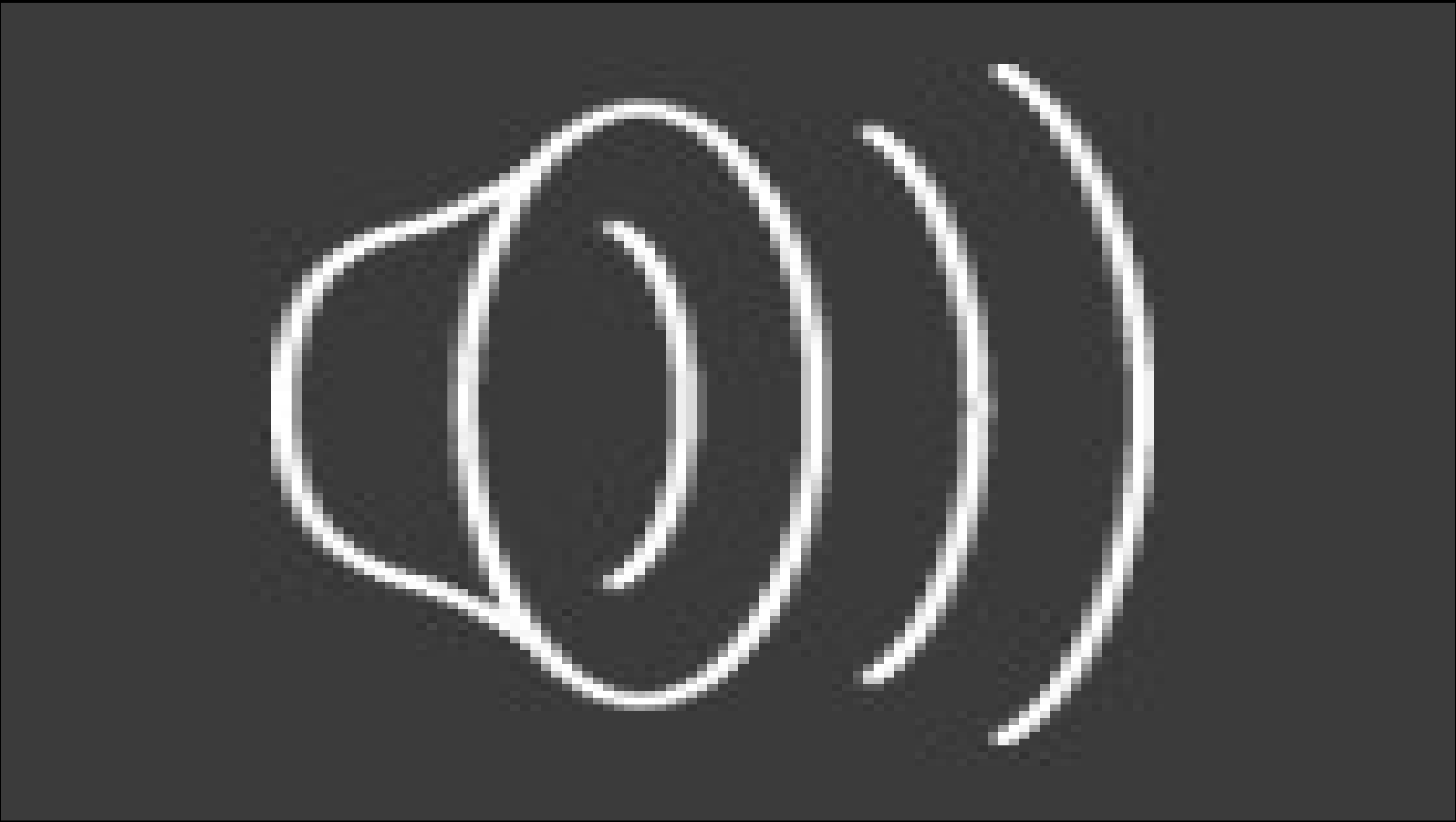

Courtesy of Villaescusa-Navarro

L=150 Mpc/h **$N_{cdm}=512^3$** **$N_\nu=1024^3$** **$z_{in}=49$**

CDM/ν clustering in high resolution simulations

(2400 times smaller than DEMNUni)

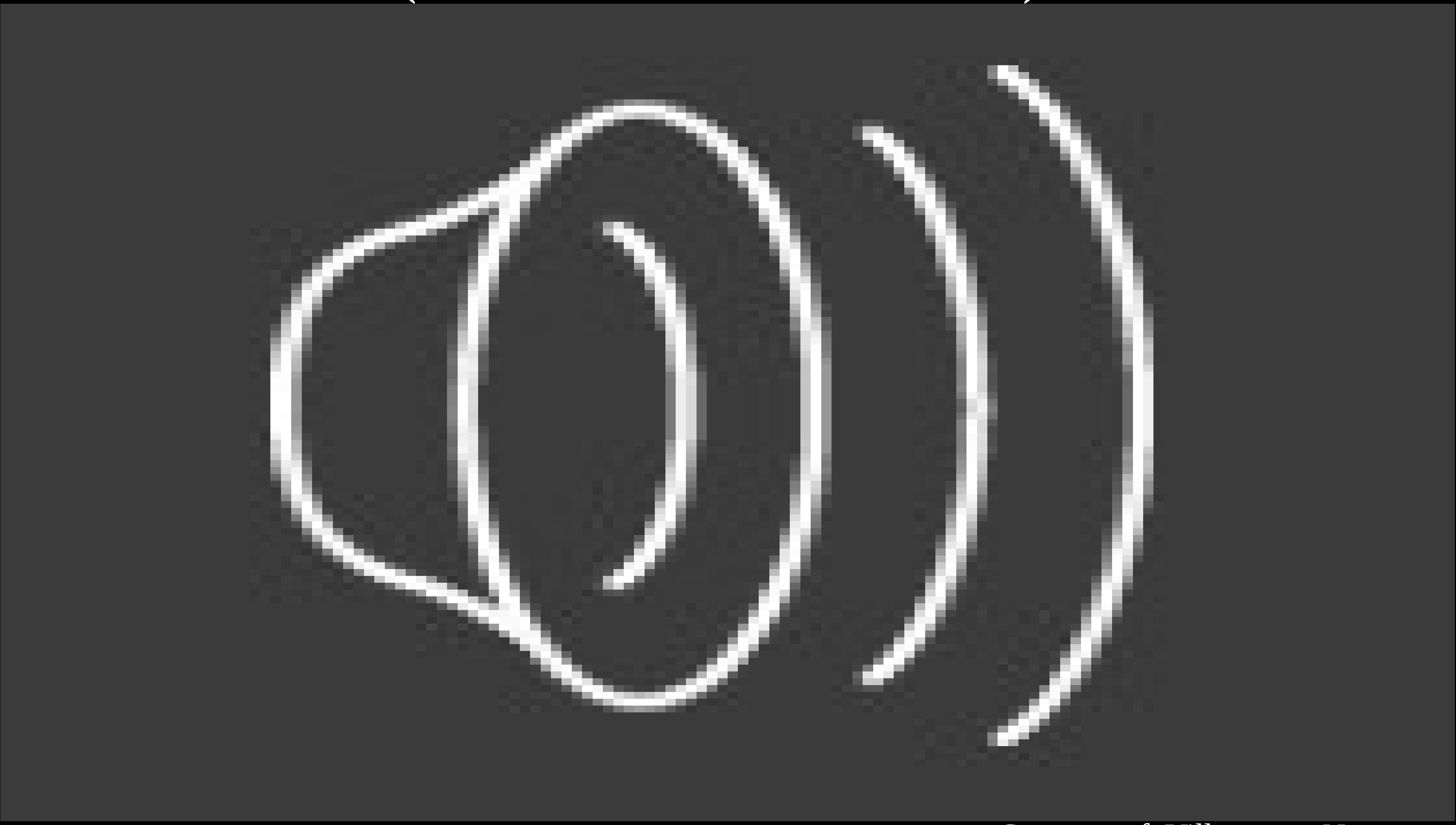

Courtesy of Villaescusa-Navarro

$L=150$ Mpc/h $N_{cdm}=512^3$ $N_{\nu}=1024^3$ $z_{in}=49$

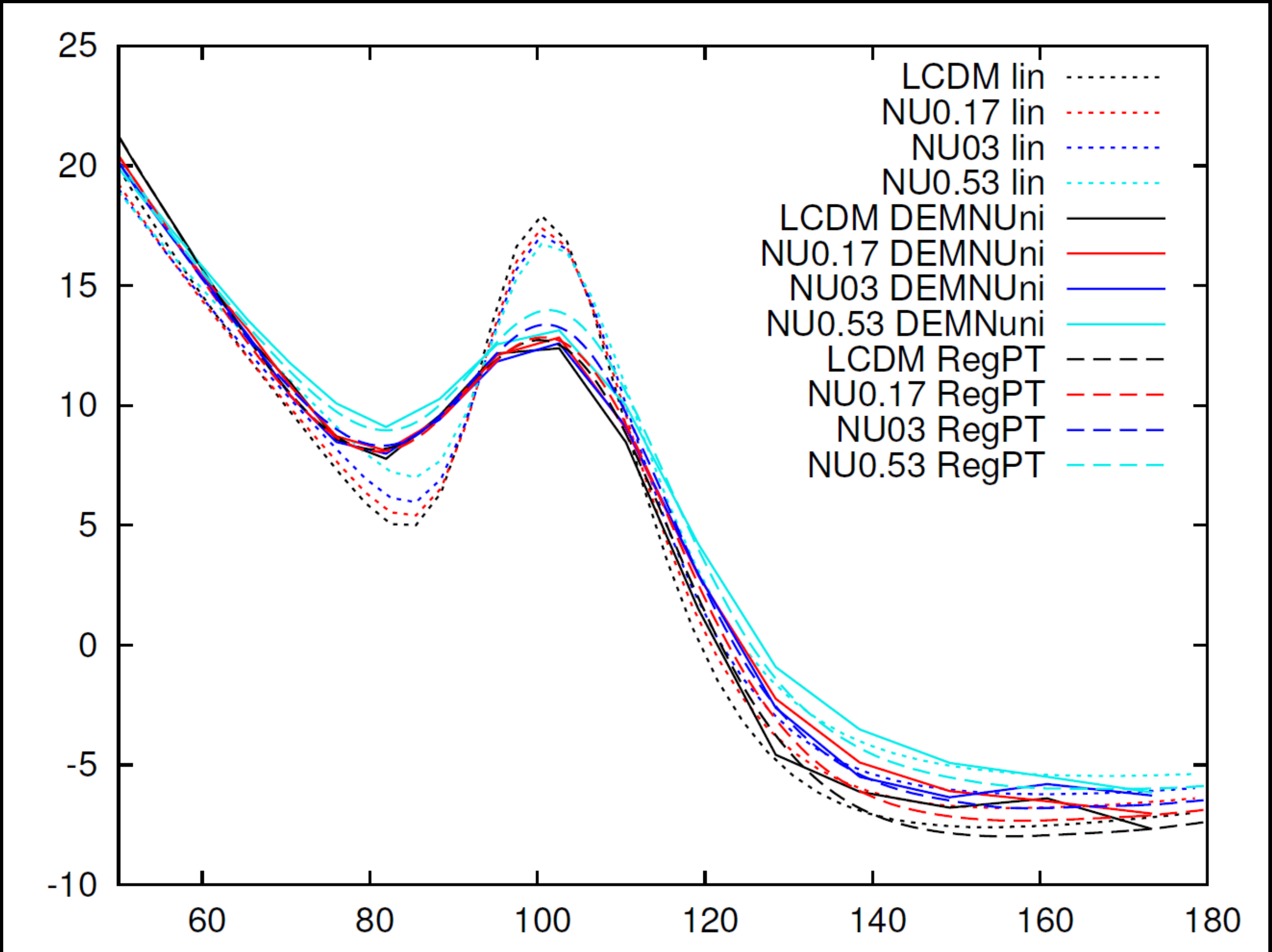

Bianchi et al work in progress

Different contributions to the total matter P(k)

Castorina, CC et al. 2015

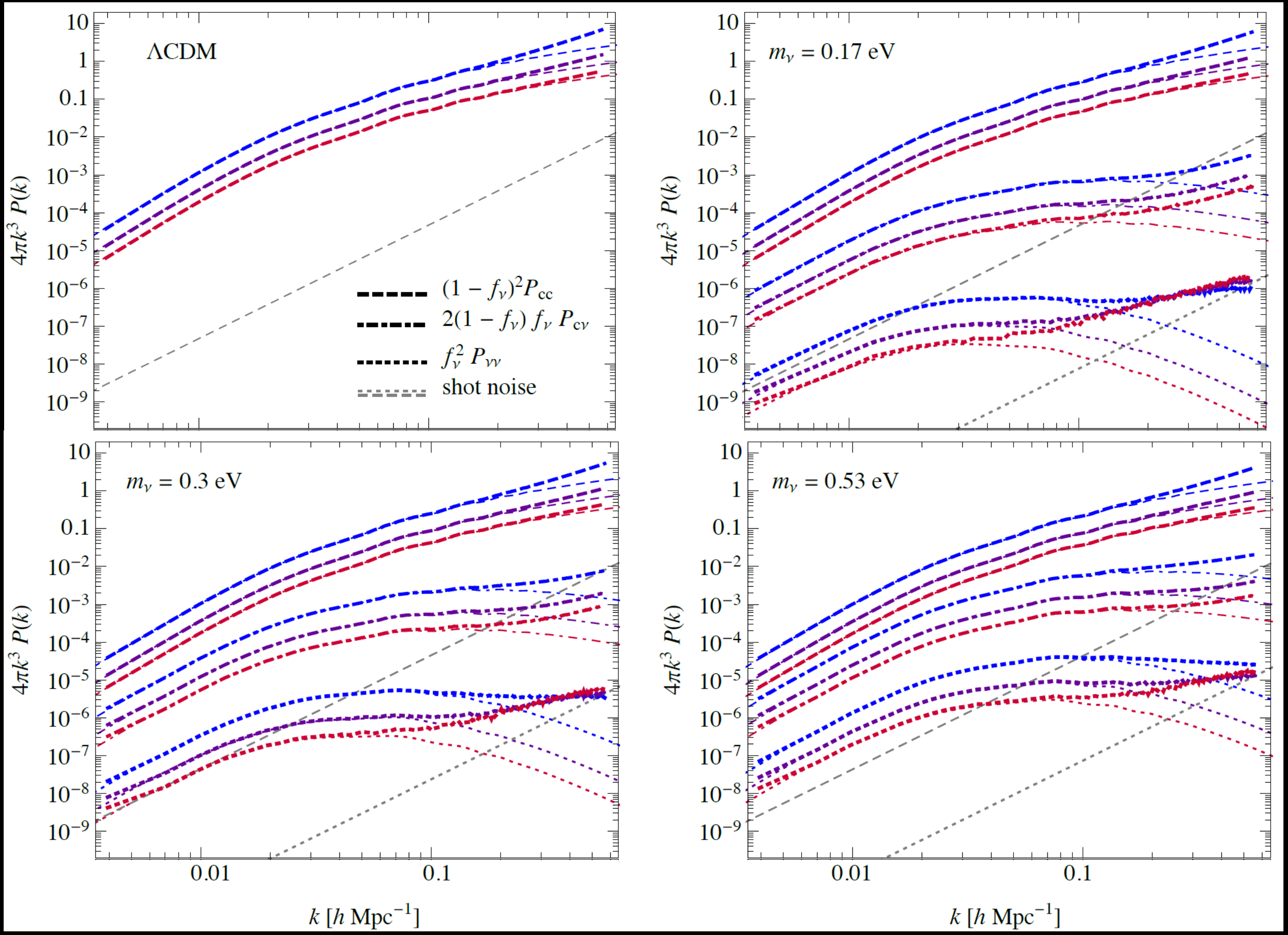

$$P_m(k;z) = (1-f_\nu)^2\, P_{cb}(k;z) + 2\,(1-f_\nu) f_\nu\, P_{cb,\nu}(k;z) + f_\nu^2\, P_\nu(k;z)$$

***$P_m(k)$* is described at the 1% level accuracy up to k=1*h*/Mpc, assuming the nonlinear evolution of CDM alone, and the linear prediction for the other components**

Perturbation theory vs Simulations

Castorina, CC et al. 2015

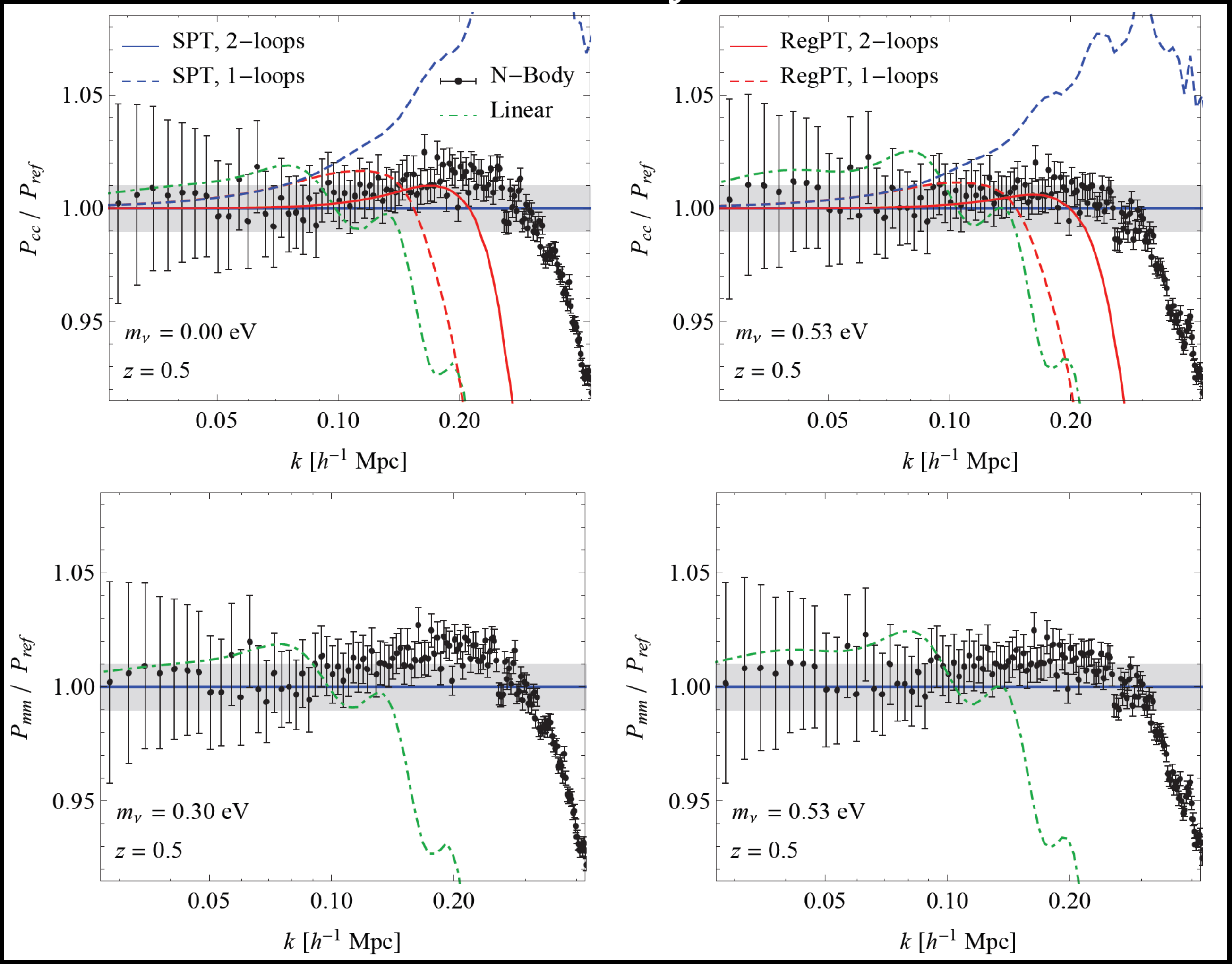

$$P^{PT}_{mm}(k) = (1 - f_\nu)^2\, P^{PT}_{cc}(k) + 2\,(1 - f_\nu)\, f_\nu\, P^L_{c\nu}(k) + f_\nu^2\, P^L_{\nu\nu}(k)$$

(RegularizedPT: Bernardeau et al 2008, Taruya et al 2012)

Here the neutrino induced scale-dependence is limited to the linear growth factor, *D(k,z)*, while the perturbation kernels are standard ones. PT works better with M_ν

Modifications to Halofit

Castorina, CC et al. 2015

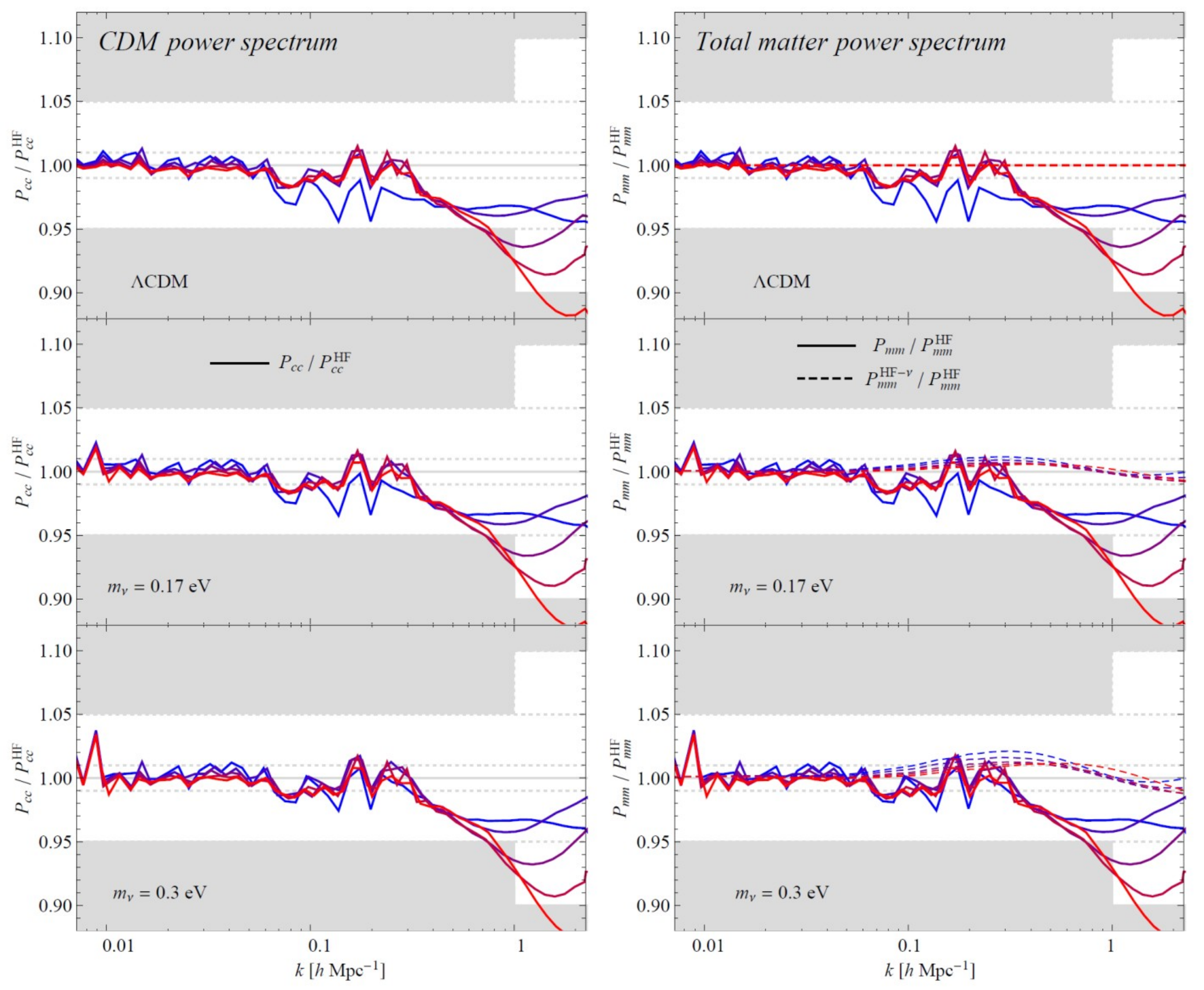

$$P_{mm}^{HF}(k) \equiv (1-f_\nu)^2\, P_{cc}^{HF}(k) + 2\, f_\nu\, (1-f_\nu)\, P_{c\nu}^{L}(k) + f_\nu^2\ P_{\nu\nu}^{L}(k)$$

$$P_{cc}^{HF}(k) \;=\; \mathcal{F}_{HF}[P_{cc}^{L}(k)]$$

HALOFIT mapping only for CDM, other contributions are assumed to be linear.
Shaded areas denote regions beyond the accurracy expected from Halofit.

Halo mass function

$$\frac{dn(M,z)}{dM} = \nu f(\nu) \frac{\rho_m}{M^2} \frac{d\ln\nu}{d\ln M}
\begin{cases}
\nu \equiv \dfrac{\delta_c}{\sigma(M,z)} \qquad \delta_c = 1.686 \\
\sigma^2(M,z) = \dfrac{1}{2\pi^2}\displaystyle\int_0^\infty k^2 P_m(k) W^2(k,R)\,dk \\
M = \dfrac{4\pi}{3}\rho_m R^3
\end{cases}$$

What about massive neutrino cosmologies?

- No prescription

$\cancel{\rho_m \quad P_m(k)}$

- Matter prescription

Brandbyge et al. 2010
Marulli et al. 2011
Villaescusa-Navarro et al. 2013

- Cold dark matter prescription

Ichiki & Takada 2011
Castorina et al. 2014
Costanzi et al. 2014
Castorina et al. 2015

Halo Mass Function: FoF

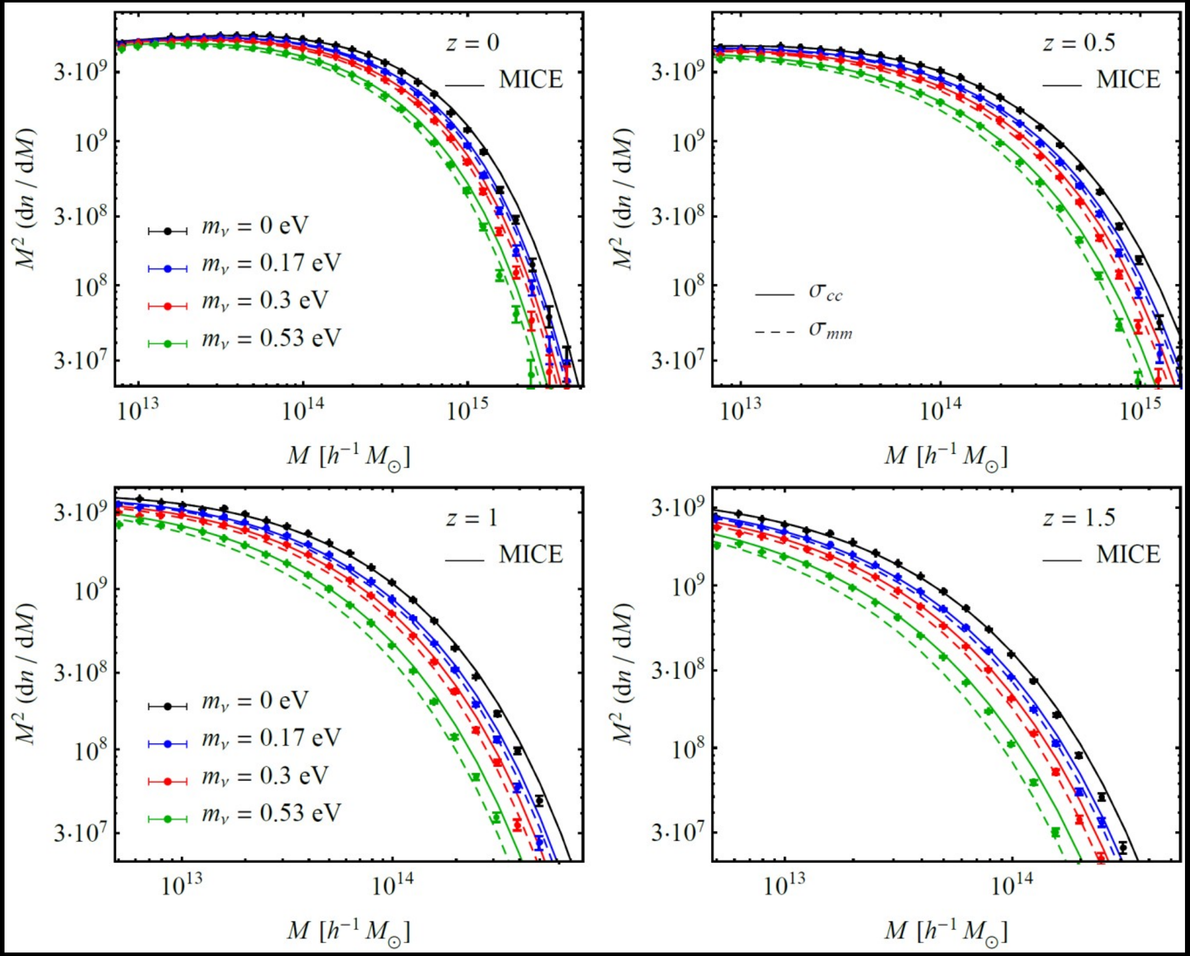

Castorina, CC et al. 2015

We recover the ρ_{cc} and σ_{cc} prescription from Ichiki&Takada (2012) and Castorina et al (2014) for the MICE formula. Note the large halo-mass range.

Halo Mass Function: FoF (MICE) vs SO (Tinker)

Castorina, CC et al. 2015

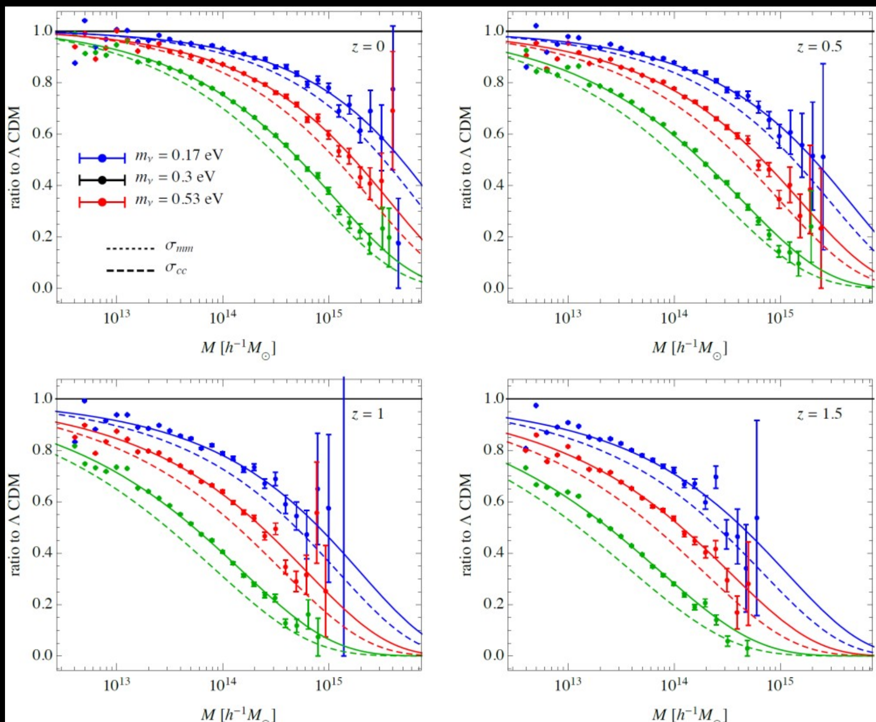

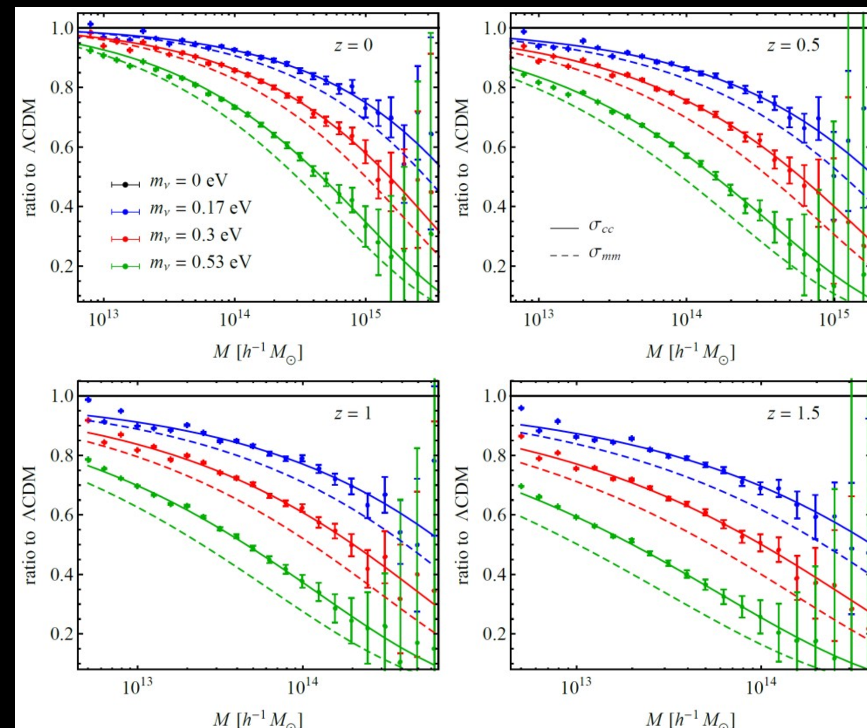

The ρ_{cc} and σ_{cc} prescriptions allow to recover the theoretical MF for both FoF and SO halos

Same conclusions for the bias

Castorina, CC et al. 2015

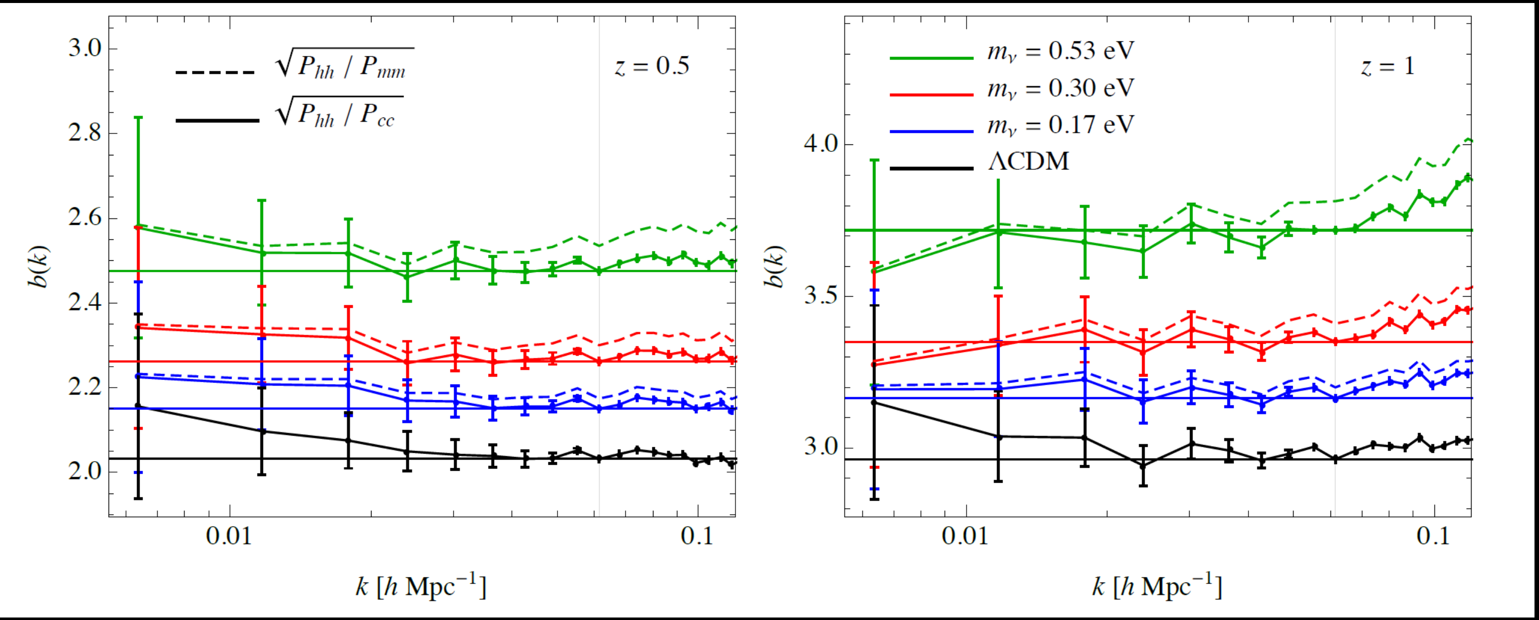

$$b_c = \sqrt{\frac{P_{hh}}{P_{cc}}}$$

$$b_m = \sqrt{\frac{P_{hh}}{P_{mm}}}$$

The σ_{cc} prescription mitigates the ν-induced scale dipendence of the bias at intermediate scales. The halo bias defined with respect to DM presents a spurious scale-dependence due to the difference between the cold and total matter power spectra.

Measurements in redshift space

Castorina, CC et al. 2015

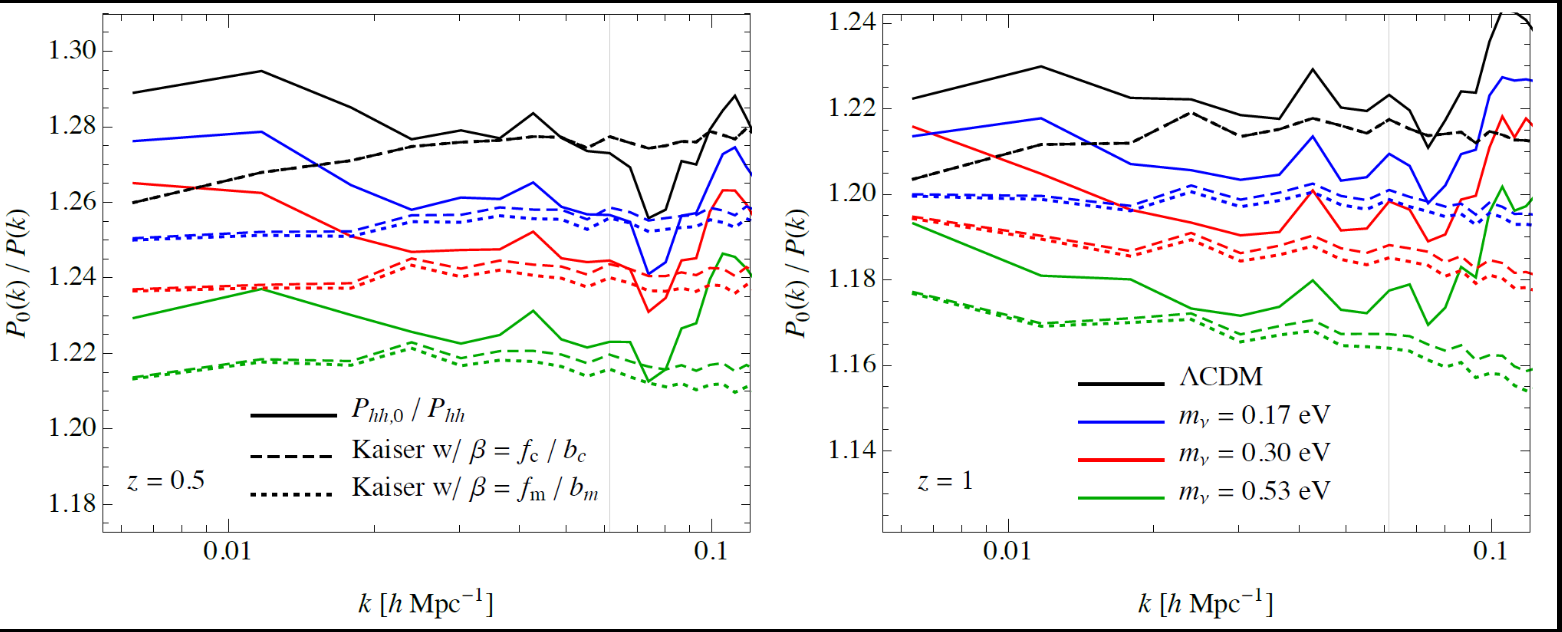

$$P_{hh,s}(\vec{k}) = (1 + \beta\mu^2)^2 \, P_{hh}(k) = \sum_{l=0,2,4} P_{hh,\ell} \, L_\ell(\mu)$$

$$P_{hh,0}(k) = \left(1 + \frac{2}{3}\beta + \frac{1}{5}\beta^2\right) P_{hh}(k)$$

$$P_{hh,2}(k) = \left(\frac{4}{3}\beta + \frac{4}{7}\beta^2\right) P_{hh}(k)$$

$$P_{hh,4}(k) = \frac{8}{35}\beta^2 P_{hh}(k),$$

f_c and σ_{cc} prescriptions work slightly better than f_m and σ_{mm} (velocity bias effects are neglected)

The scale dependent growth-rate

Using b_{m} instead of b_{cc} implies a systematic error on the determination of the growth rate at the level of 1-2%

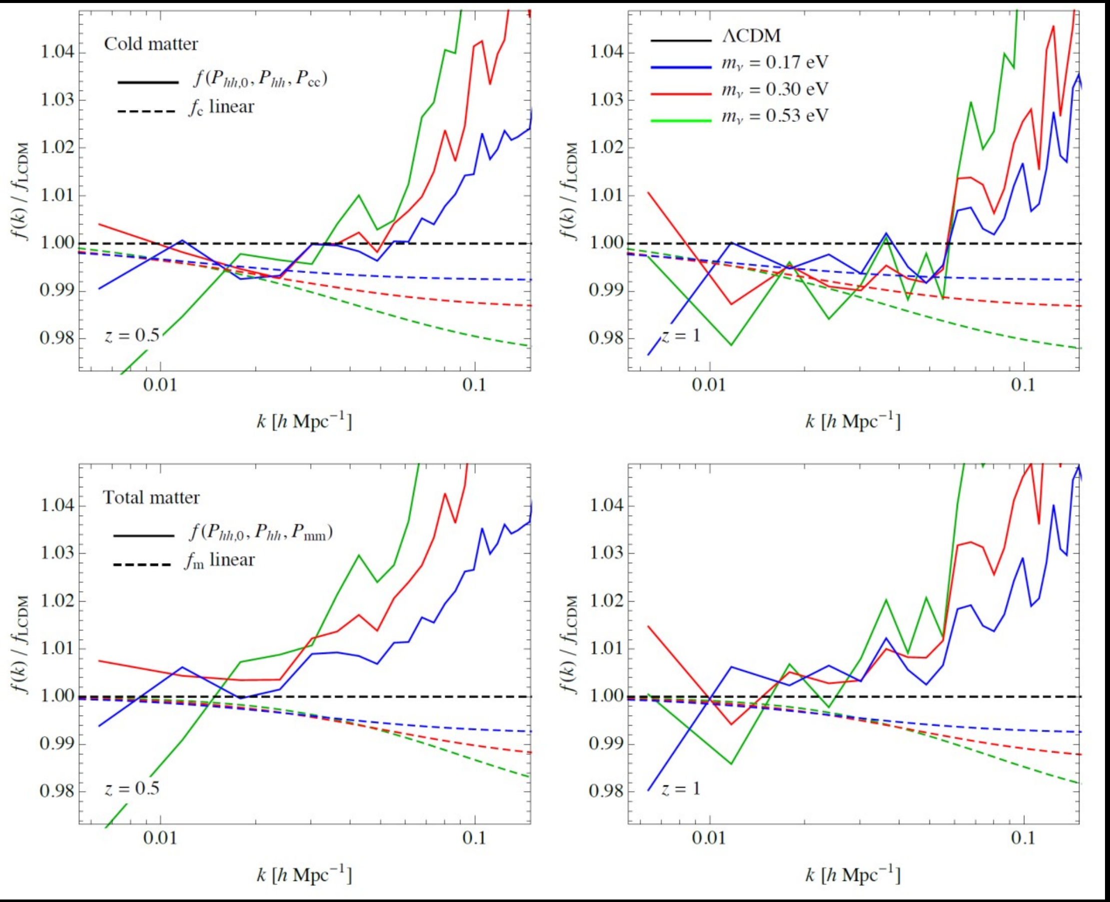

$$\beta \equiv f/b$$

$$f(a) \equiv \frac{d \ln D(a)}{d \ln a}$$

$$f(k) = \sqrt{\frac{P_{hh}(k)}{\underset{(mm)}{P_{cc}}(k)}}\,\frac{1}{3}\left[\sqrt{45\,\frac{P_{hh,0}(k)}{P_{hh}(k)} - 20} - 5\right]$$

Castorina, CC et al. 2015

Measurements in redshift space: monopole

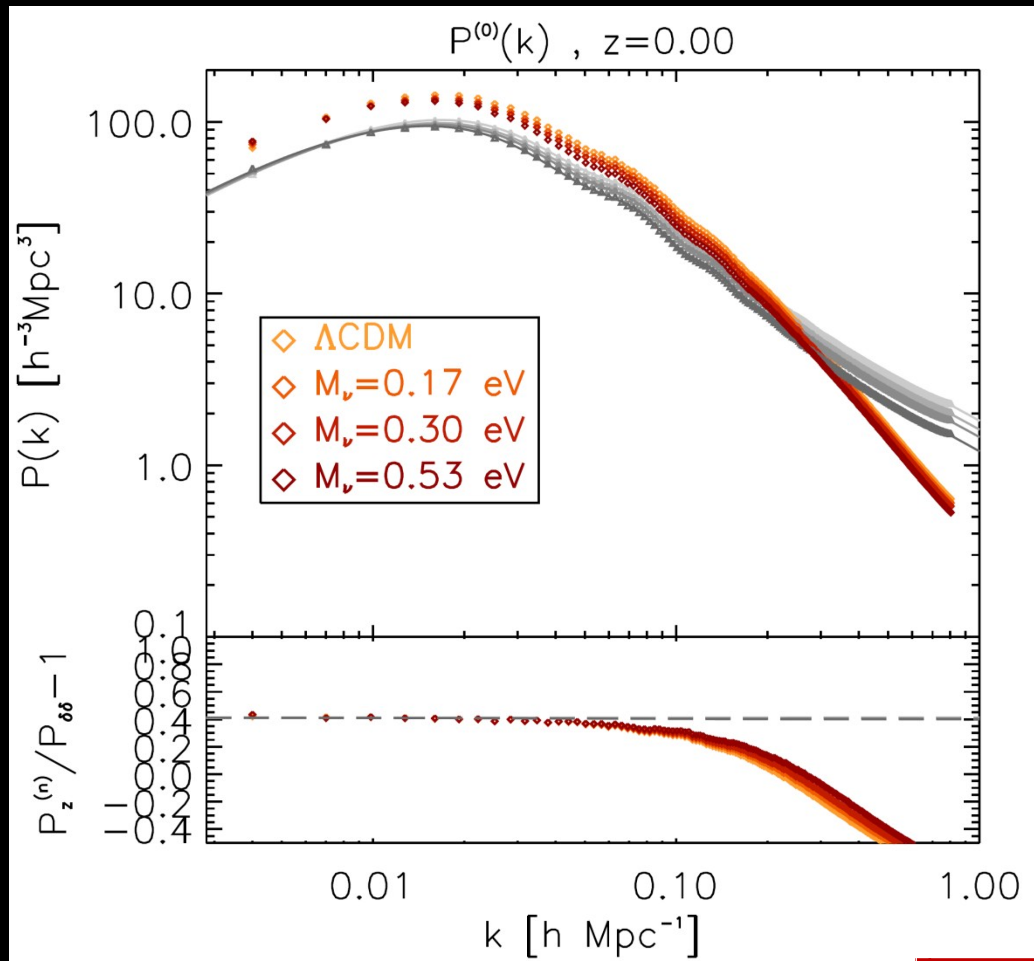

Bel , CC et al. in prep

Departures from Kaiser expectations decrease with increasing M_ν and z

$$\boxed{P_{hh,0}(k) = \left(1 + \frac{2}{3}\beta + \frac{1}{5}\beta^2\right) P_{hh}(k)}$$

$$P_{hh,2}(k) = \left(\frac{4}{3}\beta + \frac{4}{7}\beta^2\right) P_{hh}(k)$$

$$P_{hh,4}(k) = \frac{8}{35}\beta^2 P_{hh}(k),$$

Measurements in redshift space: monopole

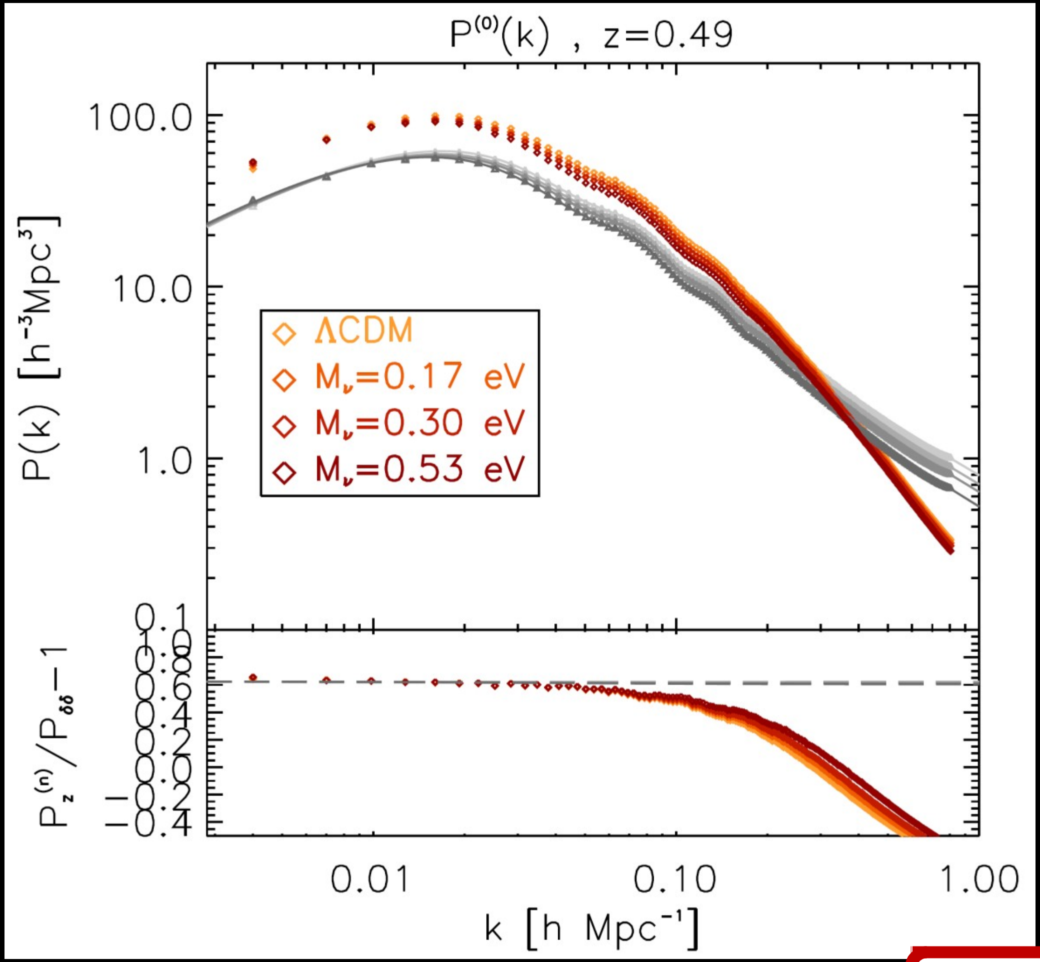

Bel , CC et al. in prep

Departures from Kaiser expectations decrease with increasing M_ν and z

$$P_{hh,0}(k) = \left(1 + \frac{2}{3}\beta + \frac{1}{5}\beta^2\right) P_{hh}(k)$$

$$P_{hh,2}(k) = \left(\frac{4}{3}\beta + \frac{4}{7}\beta^2\right) P_{hh}(k)$$

$$P_{hh,4}(k) = \frac{8}{35}\beta^2 P_{hh}(k),$$

Measurements in redshift space: monopole

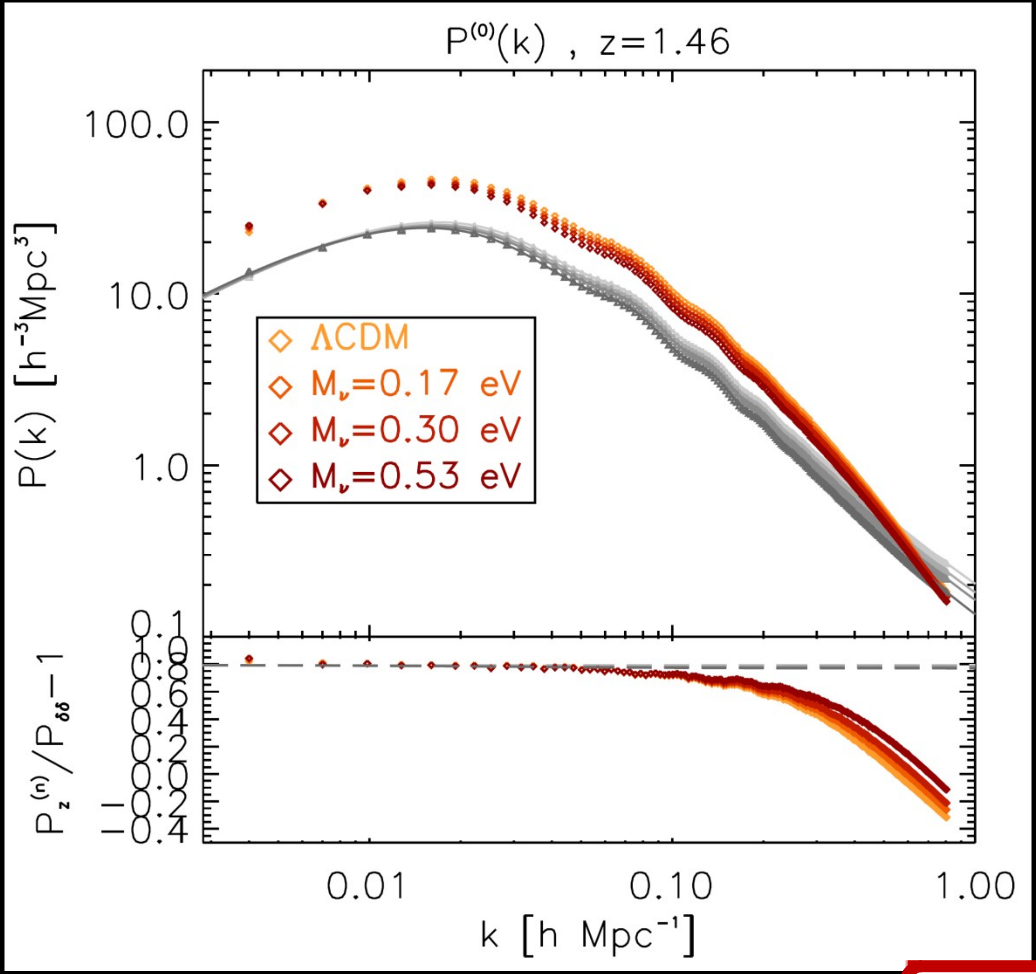

Bel , CC et al. in prep

Departures from Kaiser expectations decrease with increasing M_ν and z

$$P_{hh,0}(k) = \left(1 + \frac{2}{3}\beta + \frac{1}{5}\beta^2\right) P_{hh}(k)$$

$$P_{hh,2}(k) = \left(\frac{4}{3}\beta + \frac{4}{7}\beta^2\right) P_{hh}(k)$$

$$P_{hh,4}(k) = \frac{8}{35}\beta^2 P_{hh}(k),$$

Measurements in redshift space: monopole

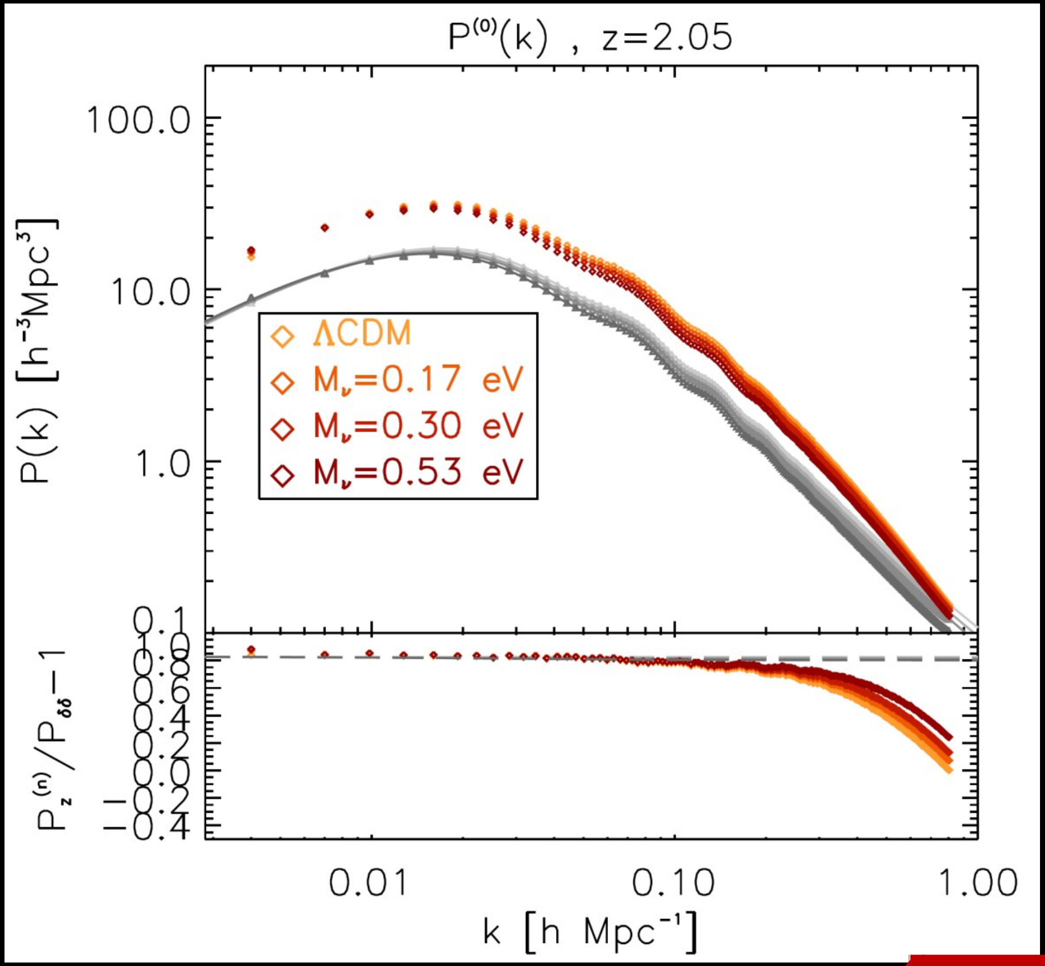

Bel , CC et al. in prep

Departures from Kaiser expectations decrease with increasing M_ν and z

$$\boxed{P_{hh,0}(k) = \left(1 + \frac{2}{3}\beta + \frac{1}{5}\beta^2\right) P_{hh}(k)}$$

$$P_{hh,2}(k) = \left(\frac{4}{3}\beta + \frac{4}{7}\beta^2\right) P_{hh}(k)$$

$$P_{hh,4}(k) = \frac{8}{35}\beta^2 P_{hh}(k),$$

Measurements in redshift space: quadrupole

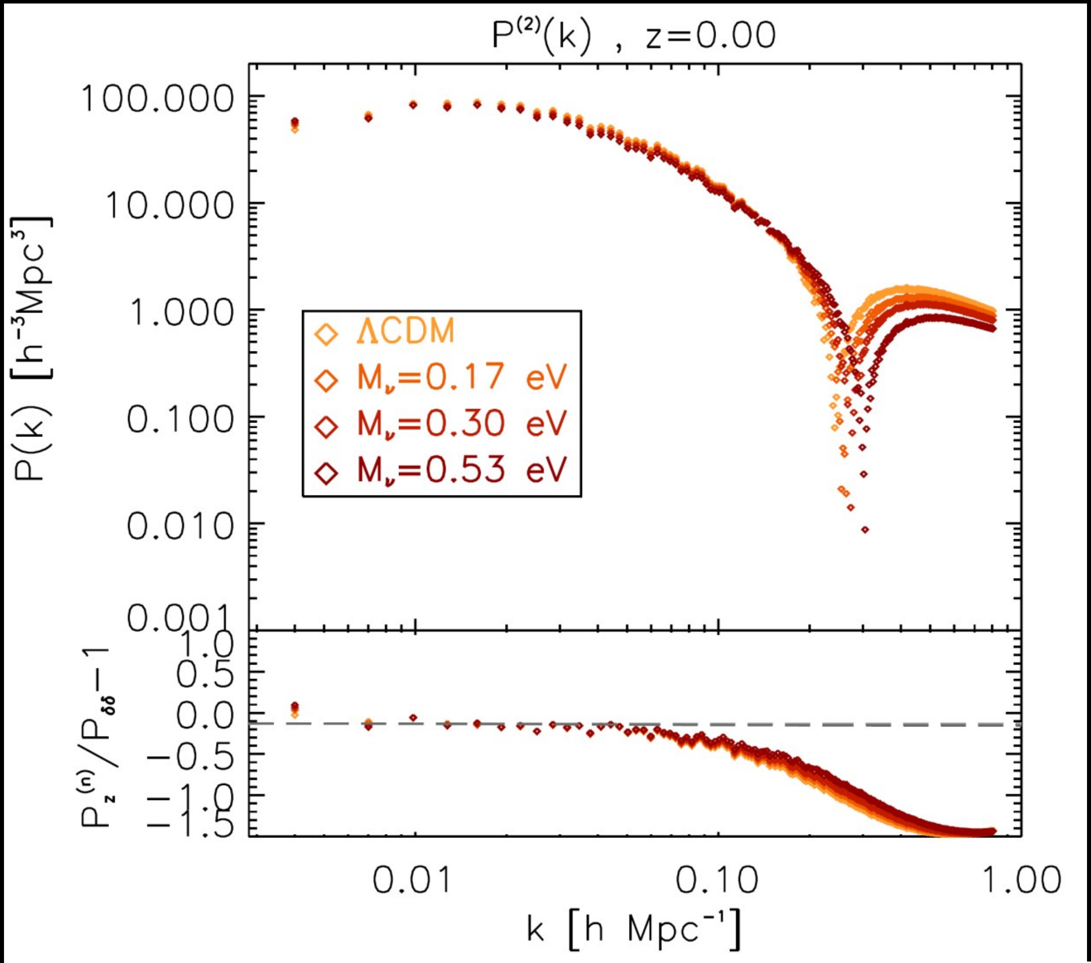

Bel , CC et al. in prep

Departures from Kaiser expectations decrease with increasing M_ν and z

$$P_{hh,0}(k) = \left(1 + \frac{2}{3}\beta + \frac{1}{5}\beta^2\right) P_{hh}(k)$$

$$\boxed{P_{hh,2}(k) = \left(\frac{4}{3}\beta + \frac{4}{7}\beta^2\right) P_{hh}(k)}$$

$$P_{hh,4}(k) = \frac{8}{35}\beta^2 P_{hh}(k),$$

Measurements in redshift space: quadrupole

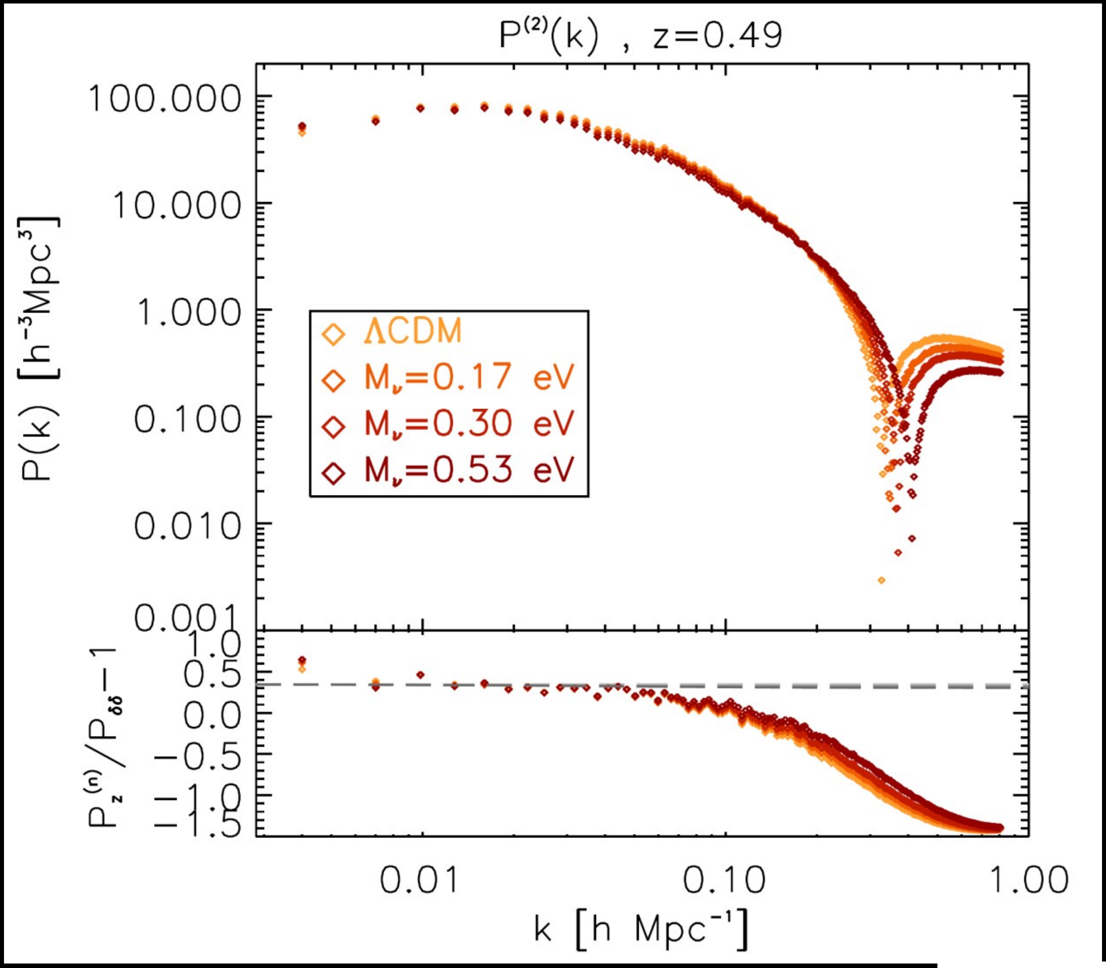

Bel , CC et al. in prep

Departures from Kaiser expectations decrease with increasing M_ν and z

$$P_{hh,0}(k) = \left(1 + \frac{2}{3}\beta + \frac{1}{5}\beta^2\right) P_{hh}(k)$$

$$\boxed{P_{hh,2}(k) = \left(\frac{4}{3}\beta + \frac{4}{7}\beta^2\right) P_{hh}(k)}$$

$$P_{hh,4}(k) = \frac{8}{35}\beta^2 P_{hh}(k),$$

Measurements in redshift space: quadrupole

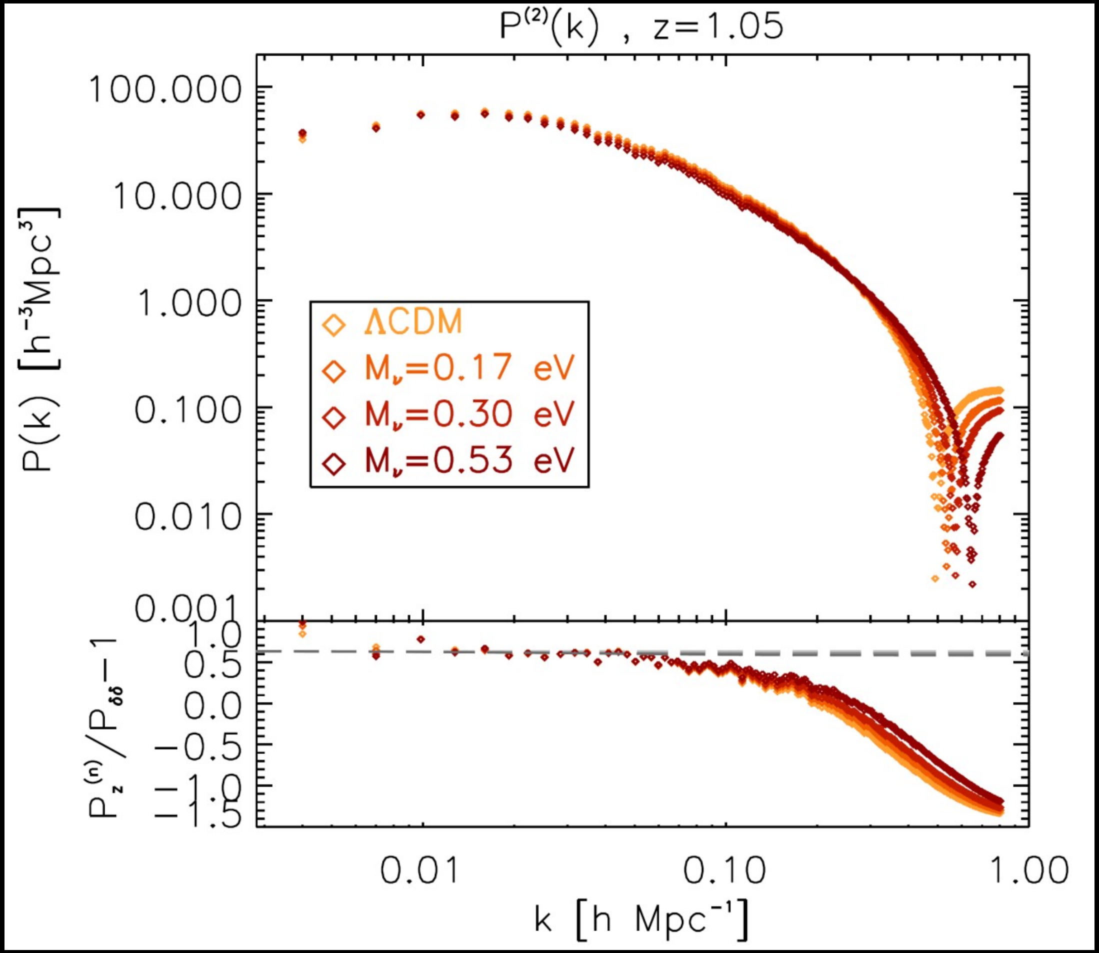

Bel , CC et al. in prep

Departures from Kaiser expectations decrease with increasing M_ν and z

$$P_{hh,0}(k) = \left(1 + \frac{2}{3}\beta + \frac{1}{5}\beta^2\right) P_{hh}(k)$$

$$\boxed{P_{hh,2}(k) = \left(\frac{4}{3}\beta + \frac{4}{7}\beta^2\right) P_{hh}(k)}$$

$$P_{hh,4}(k) = \frac{8}{35}\beta^2 P_{hh}(k),$$

Measurements in redshift space: quadrupole

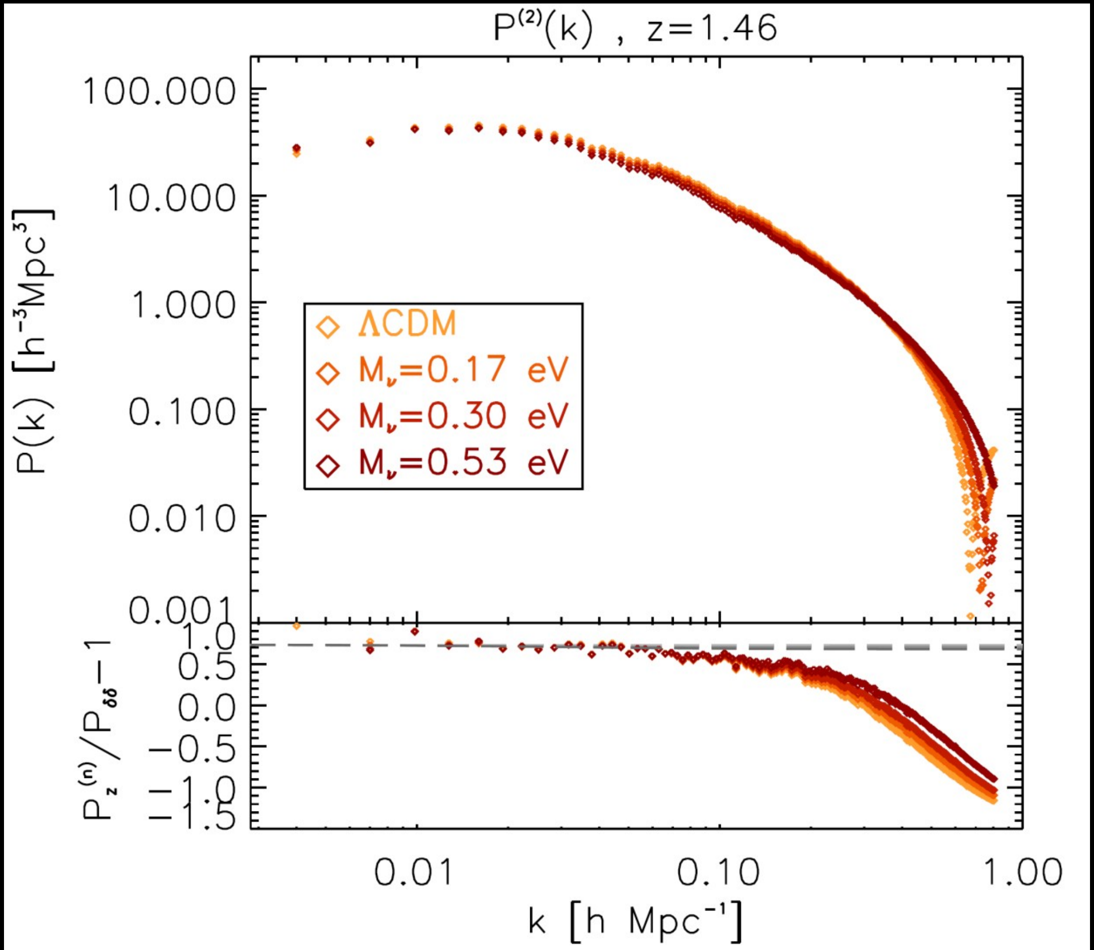

Bel , CC et al. in prep

Departures from Kaiser expectations decrease with increasing M_ν and z

$$P_{hh,0}(k) = \left(1 + \frac{2}{3}\beta + \frac{1}{5}\beta^2\right) P_{hh}(k)$$

$$\boxed{P_{hh,2}(k) = \left(\frac{4}{3}\beta + \frac{4}{7}\beta^2\right) P_{hh}(k)}$$

$$P_{hh,4}(k) = \frac{8}{35}\beta^2 P_{hh}(k),$$

Measurements in redshift space: quadrupole

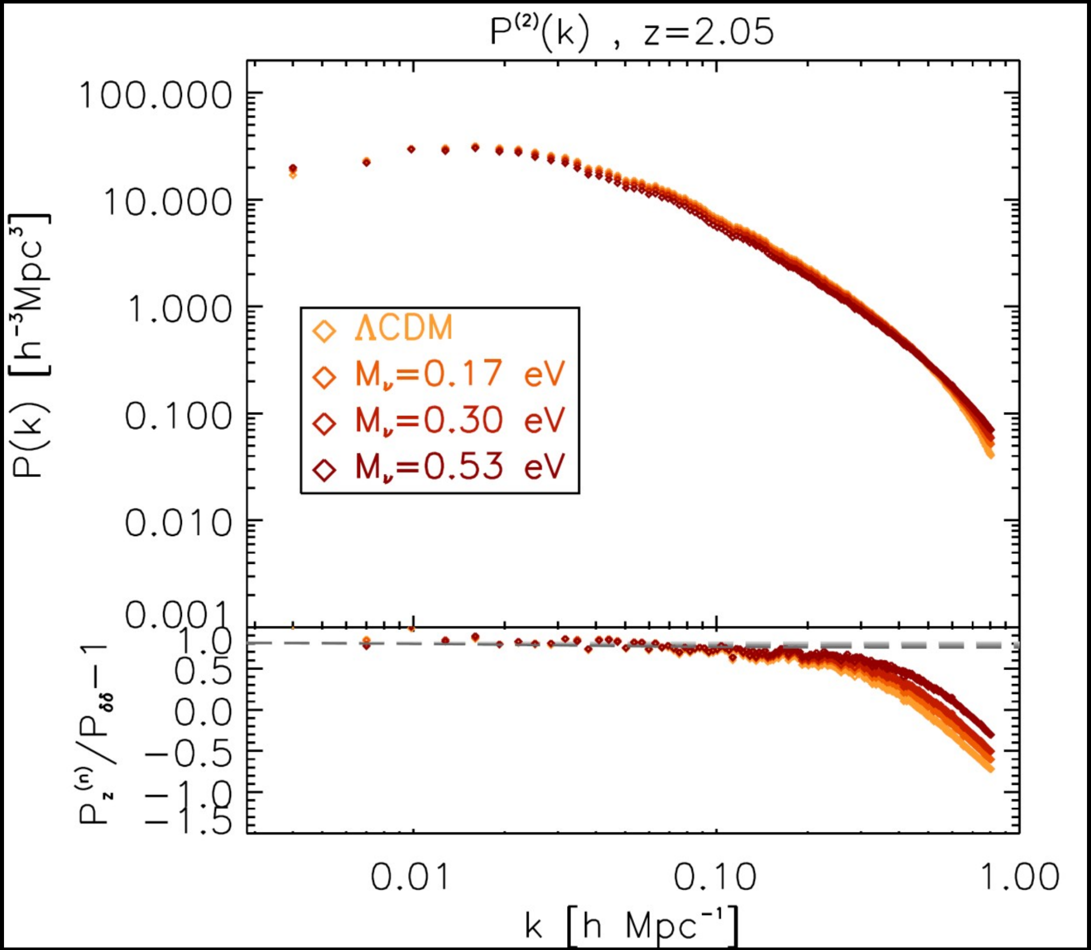

Bel , CC et al. in prep

Departures from Kaiser expectations decrease with increasing M_ν and z

$$P_{hh,0}(k) = \left(1 + \frac{2}{3}\beta + \frac{1}{5}\beta^2\right) P_{hh}(k)$$

$$\boxed{P_{hh,2}(k) = \left(\frac{4}{3}\beta + \frac{4}{7}\beta^2\right) P_{hh}(k)}$$

$$P_{hh,4}(k) = \frac{8}{35}\beta^2 P_{hh}(k),$$

Measurements in redshift space: hexadecapole

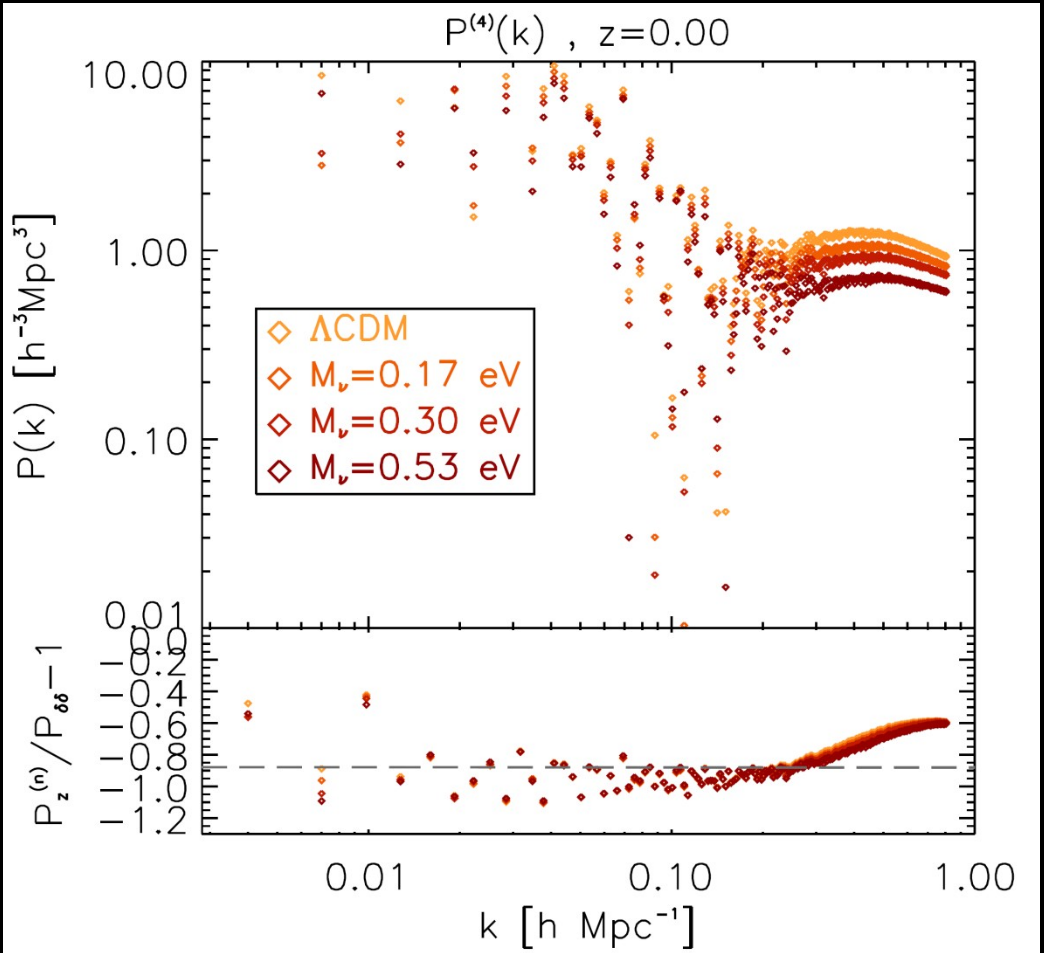

Bel , CC et al. in prep

Departures from Kaiser expectations decrease with increasing M_ν and z

$$P_{hh,0}(k) = \left(1+\frac{2}{3}\beta+\frac{1}{5}\beta^2\right)P_{hh}(k)$$

$$P_{hh,2}(k) = \left(\frac{4}{3}\beta+\frac{4}{7}\beta^2\right)P_{hh}(k)$$

$$\boxed{P_{hh,4}(k) = \frac{8}{35}\beta^2 P_{hh}(k),}$$

Measurements in redshift space: hexadecapole

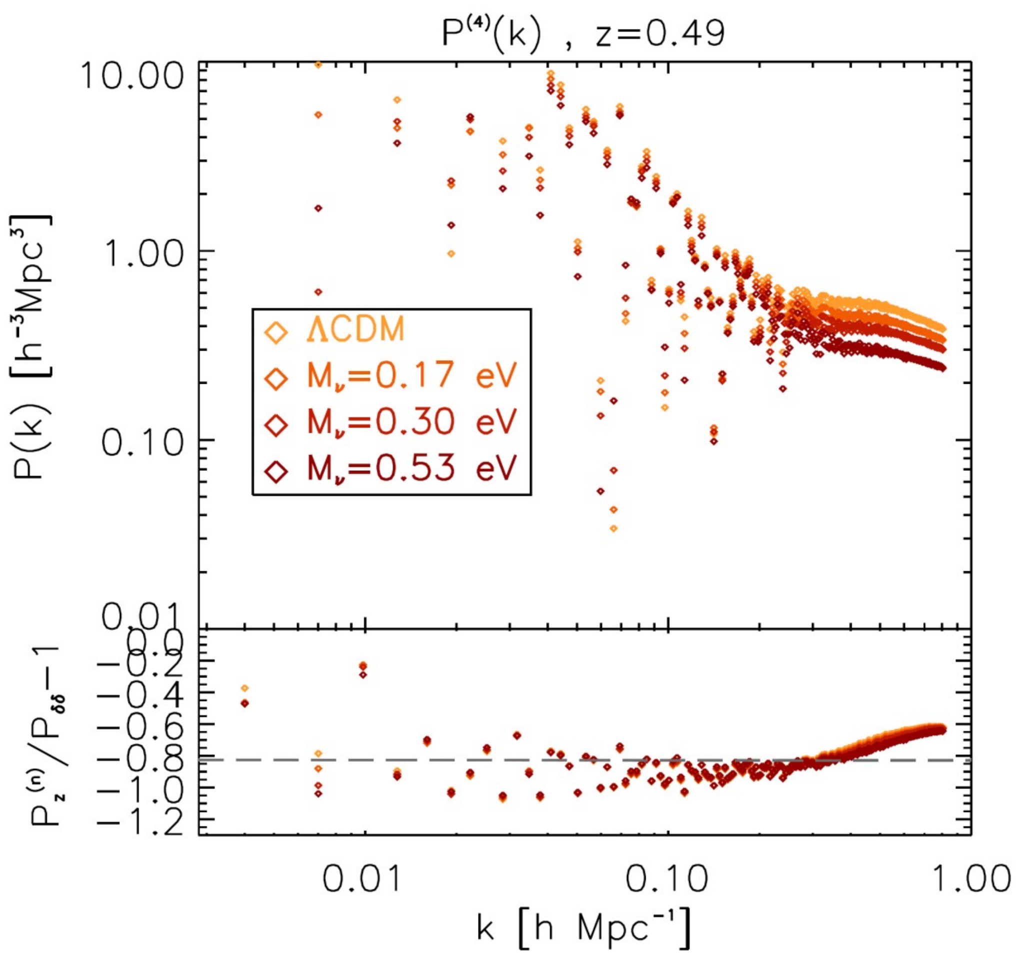

Bel , CC et al. in prep

Departures from Kaiser expectations decrease with increasing M_ν and z

$$P_{hh,0}(k) = \left(1 + \frac{2}{3}\beta + \frac{1}{5}\beta^2\right) P_{hh}(k)$$

$$P_{hh,2}(k) = \left(\frac{4}{3}\beta + \frac{4}{7}\beta^2\right) P_{hh}(k)$$

$$\boxed{P_{hh,4}(k) = \frac{8}{35}\beta^2 P_{hh}(k),}$$

Measurements in redshift space: hexadecapole

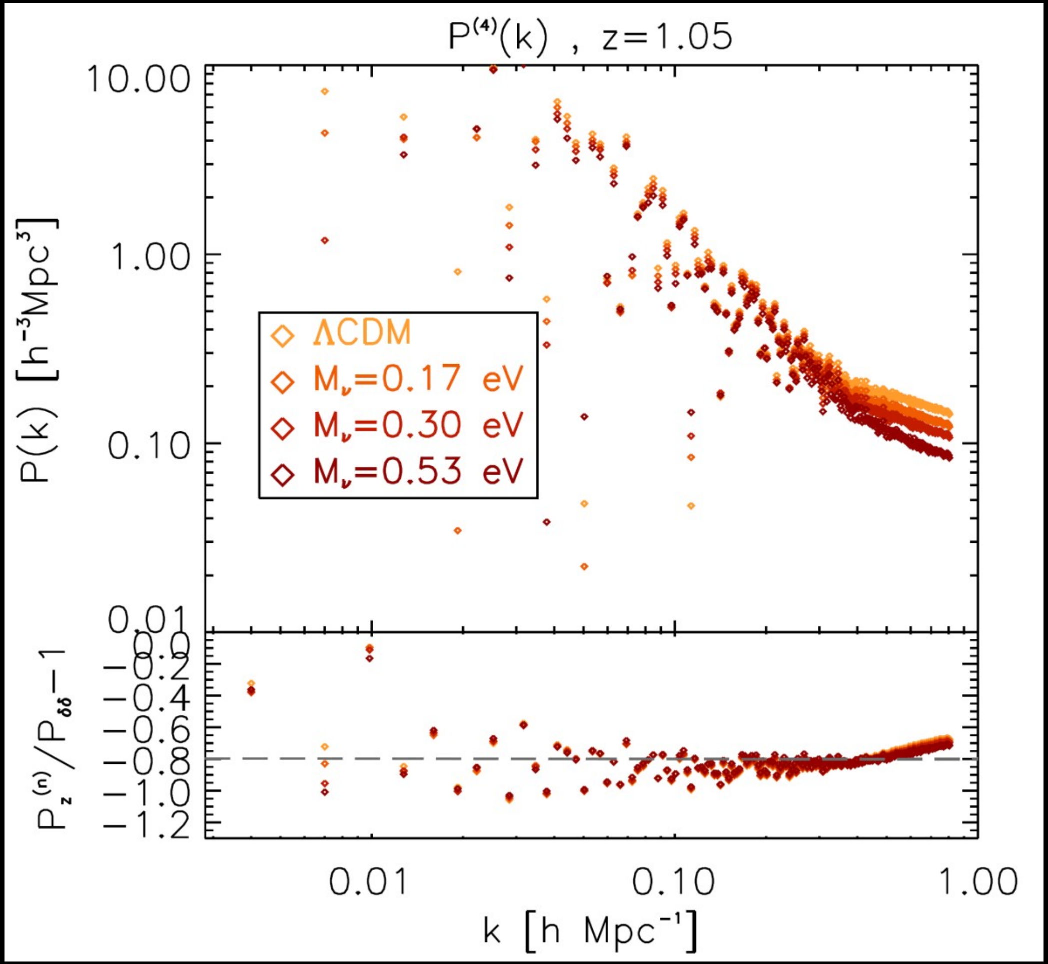

Bel , CC et al. in prep

Departures from Kaiser expectations decrease with increasing M_ν and z

$$P_{hh,0}(k) = \left(1 + \frac{2}{3}\beta + \frac{1}{5}\beta^2\right) P_{hh}(k)$$

$$P_{hh,2}(k) = \left(\frac{4}{3}\beta + \frac{4}{7}\beta^2\right) P_{hh}(k)$$

$$\boxed{P_{hh,4}(k) = \frac{8}{35}\beta^2 P_{hh}(k),}$$

Measurements in redshift space: hexadecapole

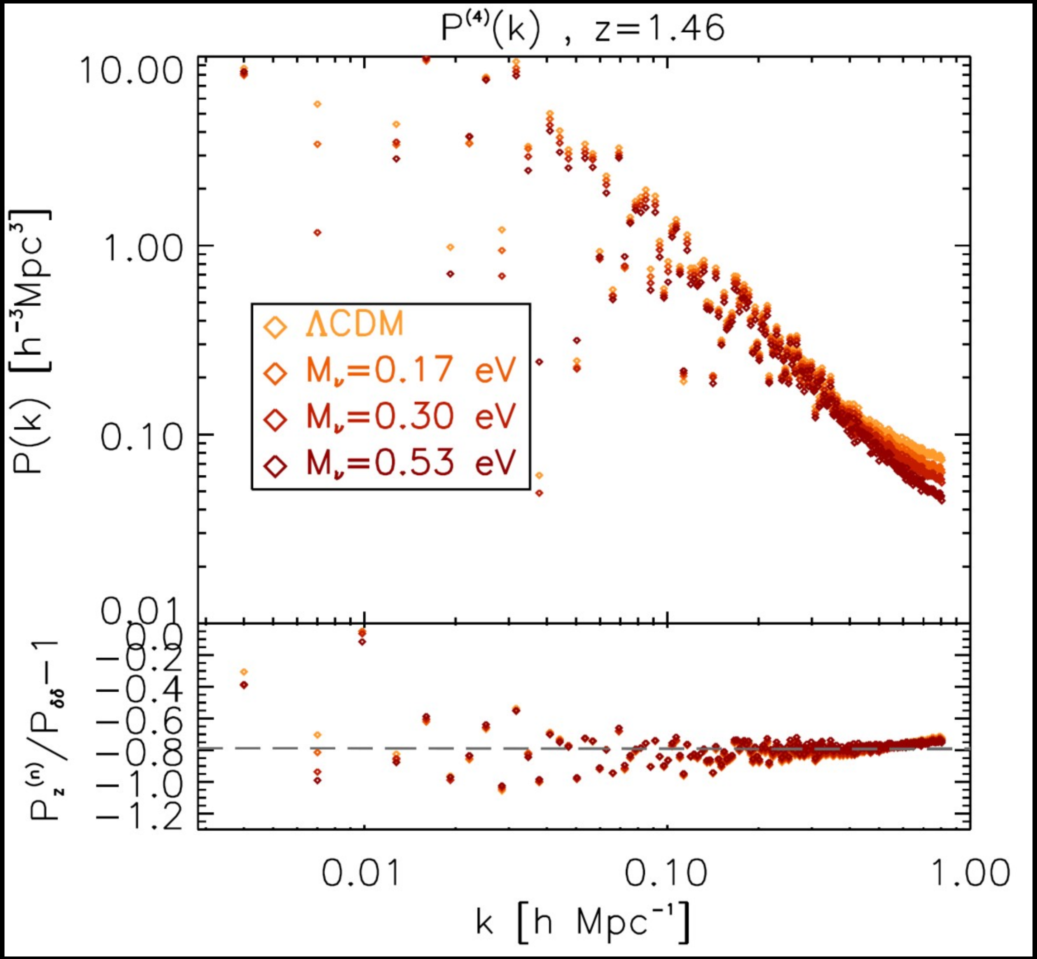

Bel , CC et al. in prep

Departures from Kaiser expectations decrease with increasing M_ν and z

$$P_{hh,0}(k) = \left(1+\frac{2}{3}\beta+\frac{1}{5}\beta^2\right)P_{hh}(k)$$

$$P_{hh,2}(k) = \left(\frac{4}{3}\beta+\frac{4}{7}\beta^2\right)P_{hh}(k)$$

$$\boxed{P_{hh,4}(k) = \frac{8}{35}\beta^2 P_{hh}(k),}$$

Measurements in redshift space: hexadecapole

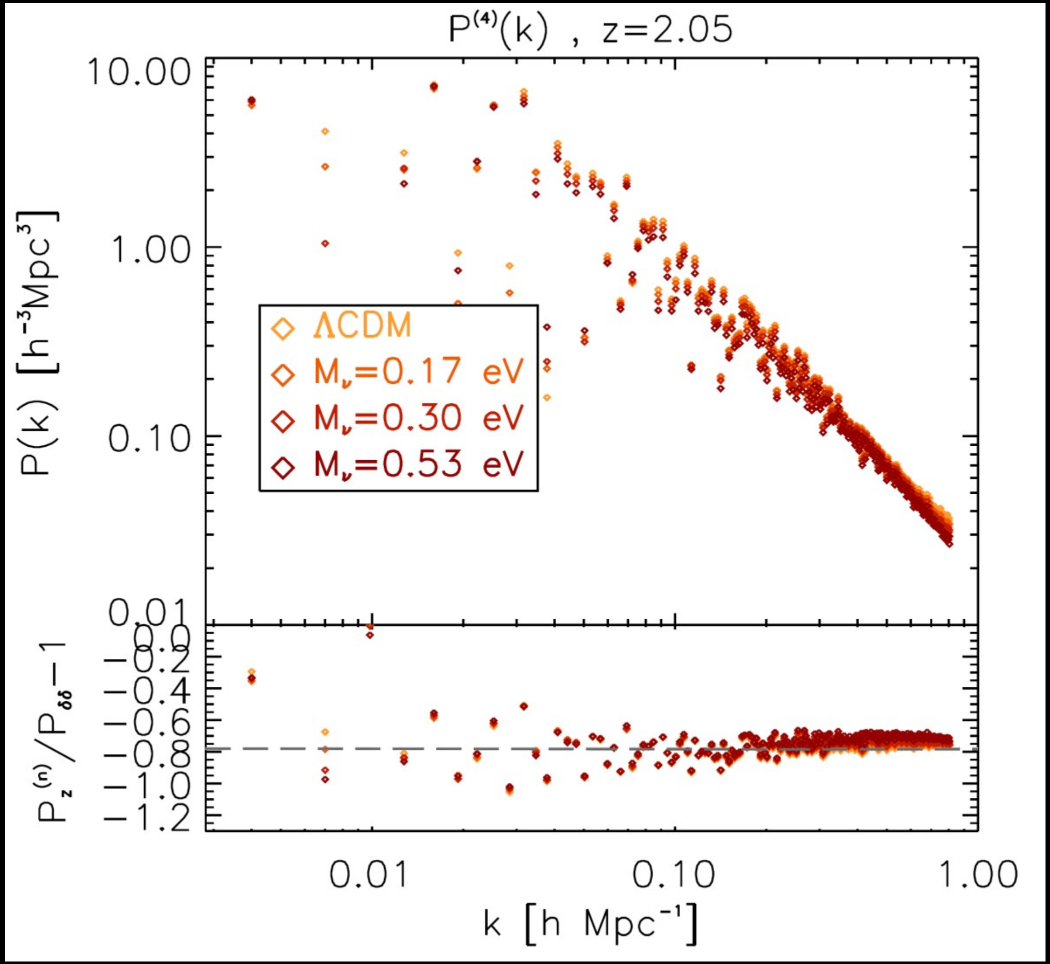

Bel , CC et al. in prep

Departures from Kaiser expectations decrease with increasing M_ν and z

$$P_{hh,0}(k) = \left(1 + \frac{2}{3}\beta + \frac{1}{5}\beta^2\right) P_{hh}(k)$$

$$P_{hh,2}(k) = \left(\frac{4}{3}\beta + \frac{4}{7}\beta^2\right) P_{hh}(k)$$

$$\boxed{P_{hh,4}(k) = \frac{8}{35}\beta^2 P_{hh}(k),}$$

Lensing and ISW-RS quantities

$$\Psi(\hat{\mathbf{n}}) \equiv -2\int_0^{r_*} \frac{r_* - r}{r_* r}\,\frac{\Phi(r\hat{\mathbf{n}};\eta_0 - r)}{c^2}\,\mathrm{d}r$$

Lensing potential in the small-angle scattering limit (Born approximation)

r= comoving distance from the observer

$$\Delta T(\hat{n}) = \frac{2}{c^3}\bar{T}_0 \int_0^{r_{\mathrm{L}}} \dot{\Phi}(r,\hat{n})\, a\, dr,$$

Total ISW-RS effect

$$\widetilde{X}(\hat{\mathbf{n}}) = X(\hat{\mathbf{n}} + \nabla\psi(\hat{\mathbf{n}}))$$

$$X = T, Q, U$$

Gradients in the grav. potential generated by LSS cause deviations in the CMB photon propagation from LS to us:

points in a direction **n**` actually come from points on the last scattering surface in a displaced direction **n**`= **n** $+\nabla\psi$

Deflection angle maps for z_s=1

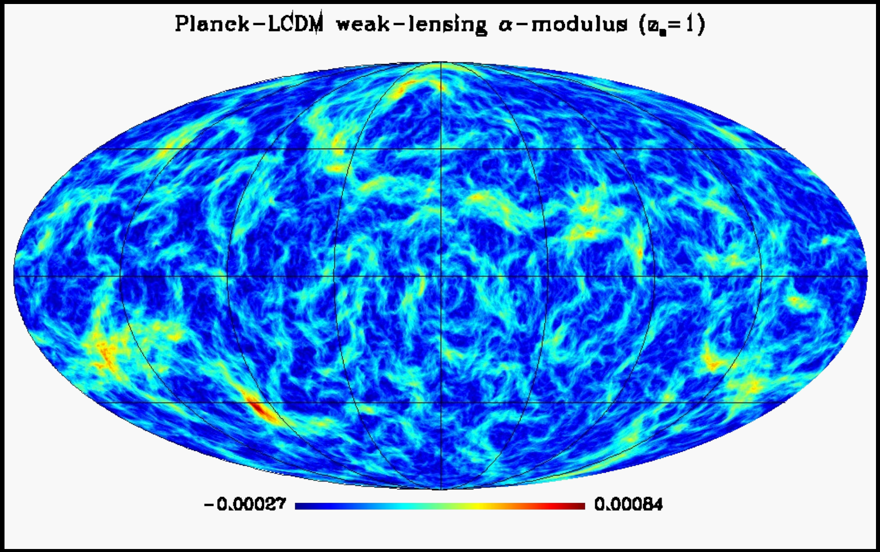

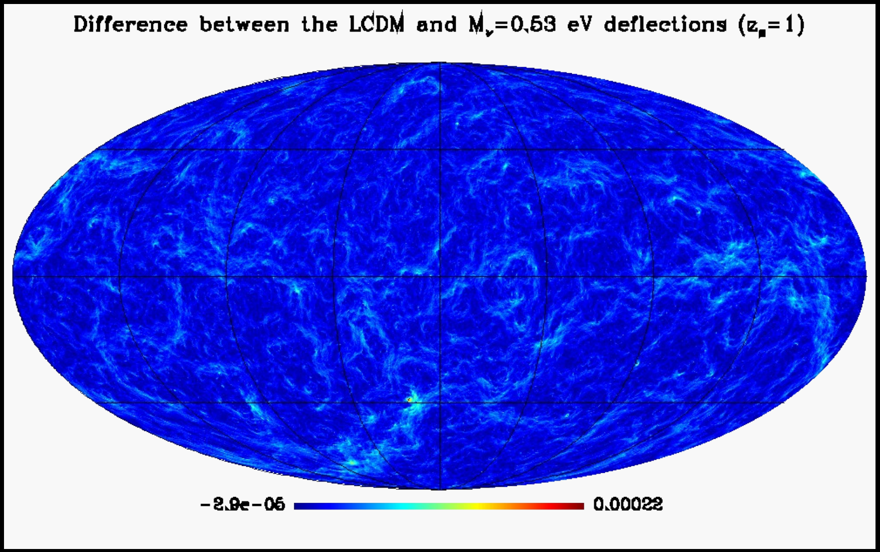

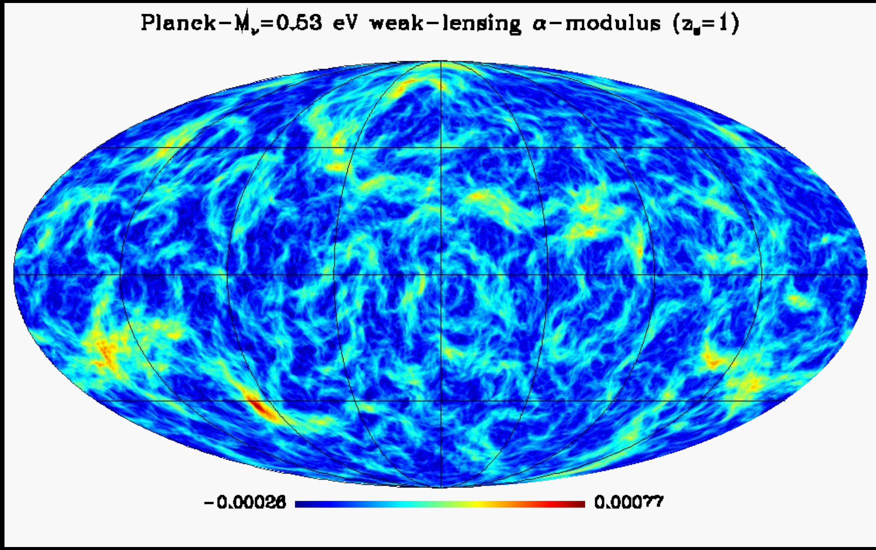

CC et al. 2016

Weak-lensing angular power spectra at different redshifts

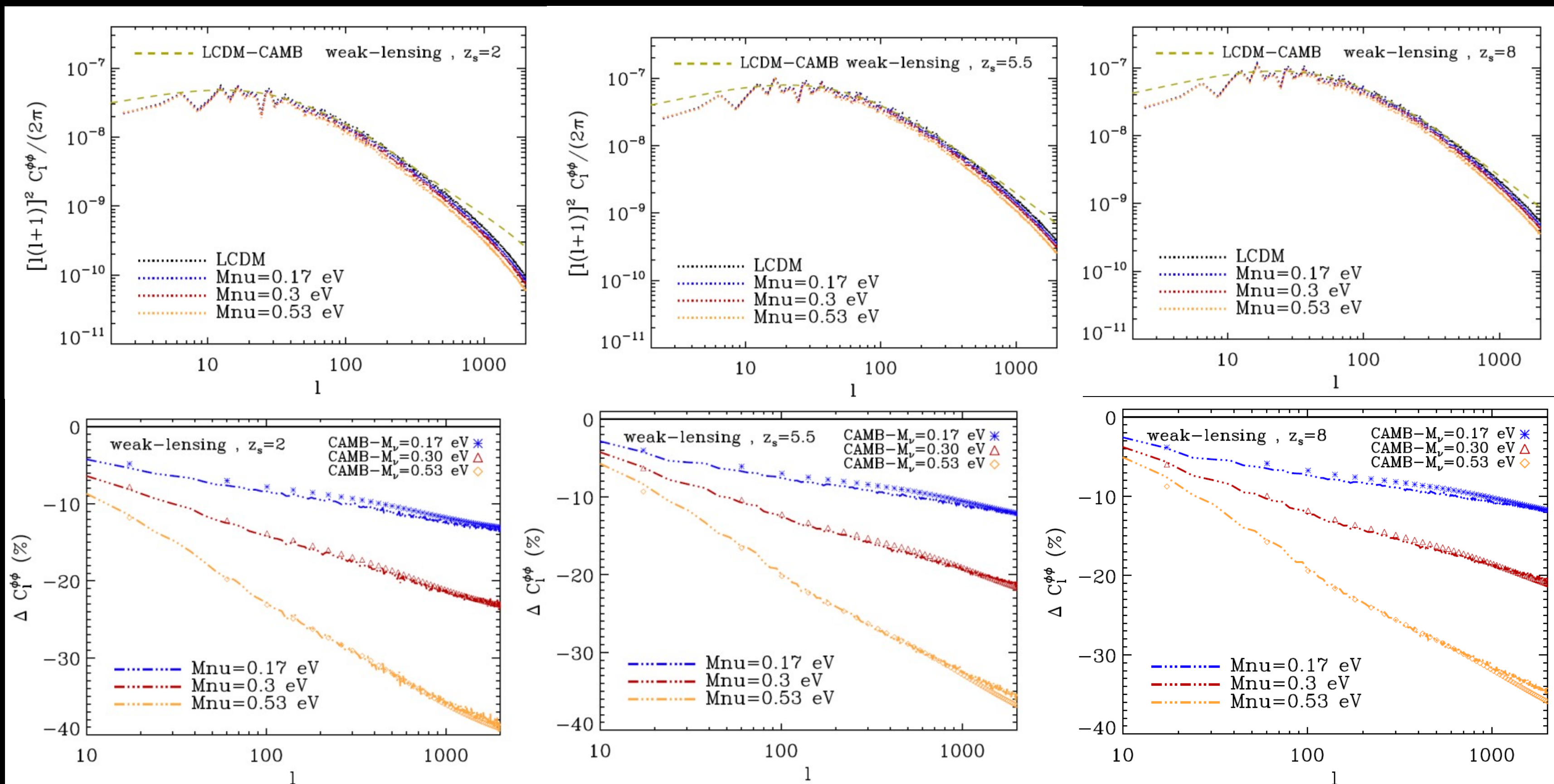

CC et al. 2016

Lack of power on small scales due to grid resolution.
The neutrino damping effect is correctely recovered up to *l*=2000

CMB-lensing angular power spectra

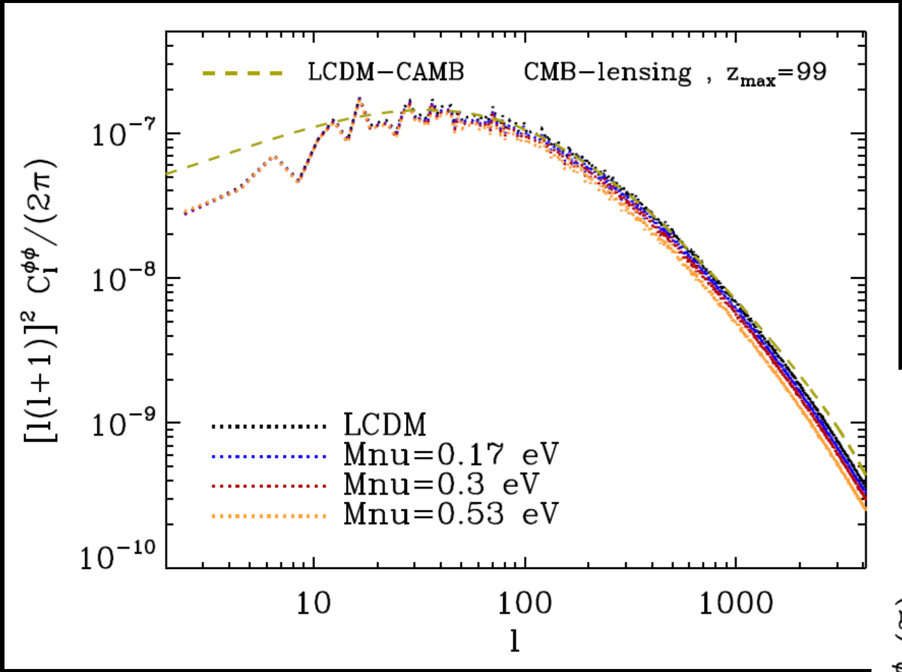

Power suppression is less than in the weak-lensing case since there is the contribution from higher z

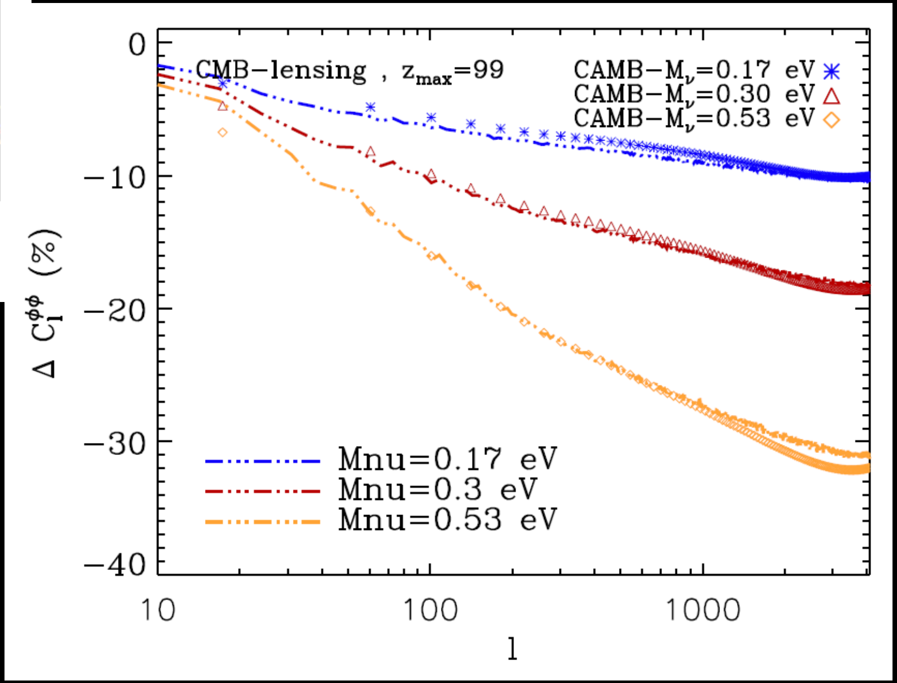

CC et al. 2016

CMB-lensing vs ISW/Rees-Sciama

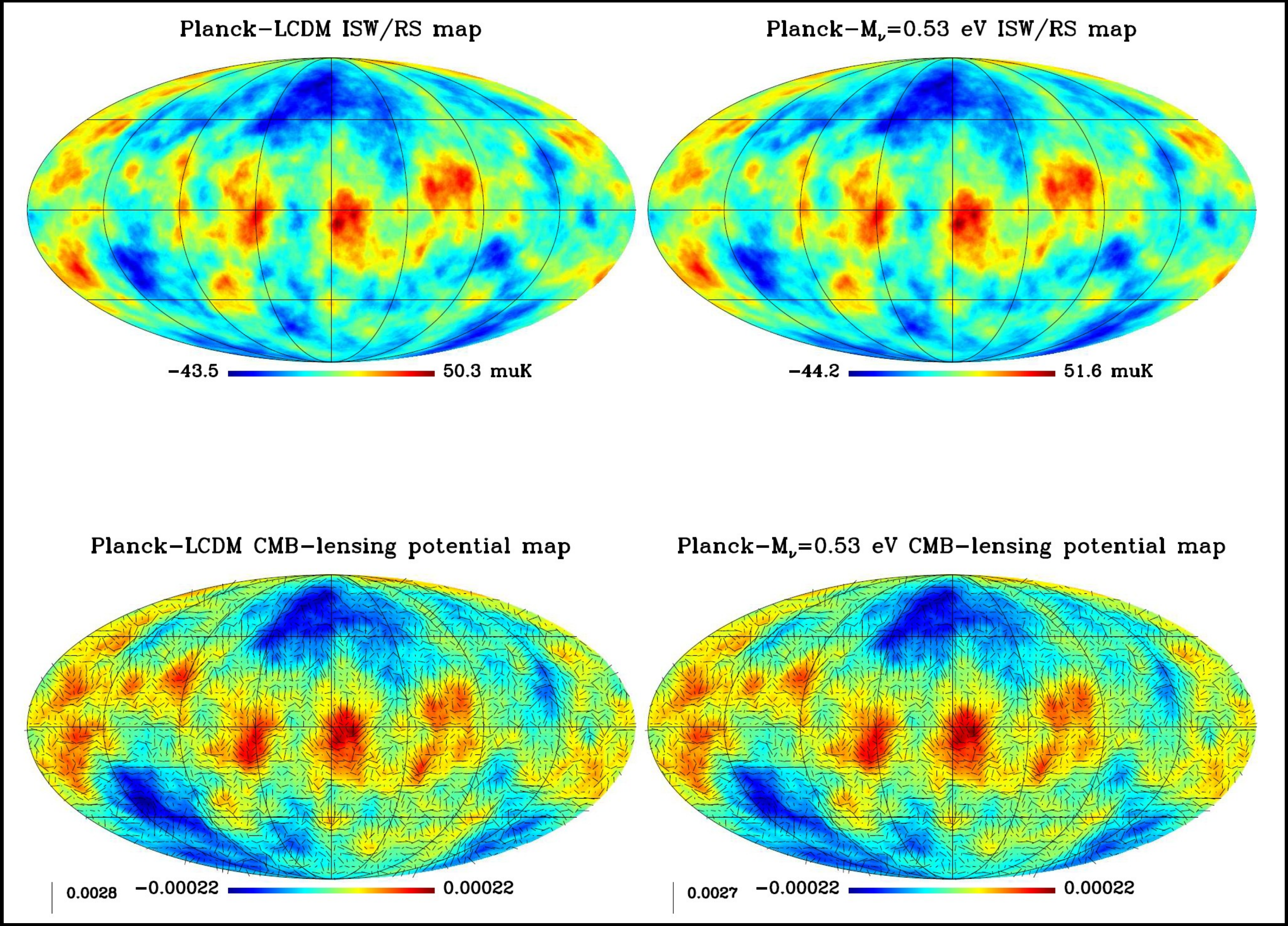

CC et al. 2016

ISW/Rees-Sciama angular power spectra

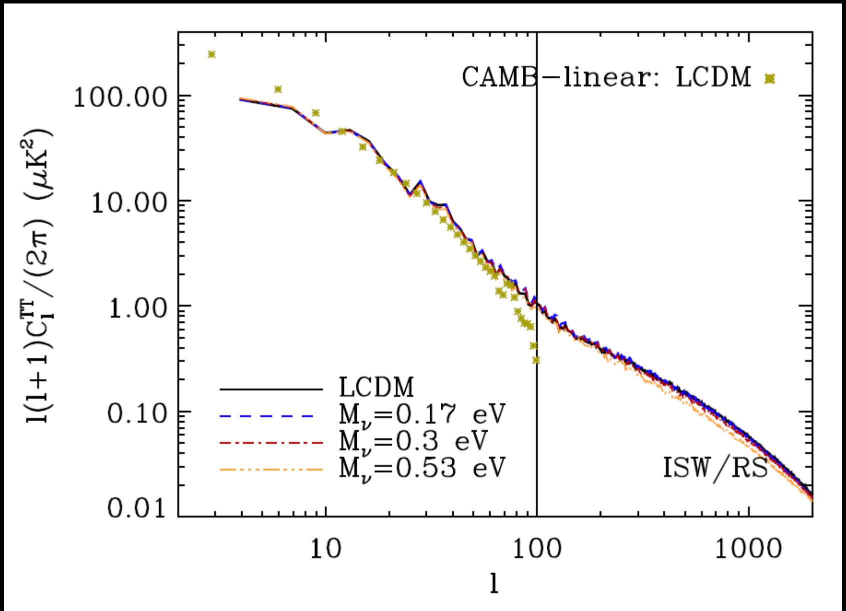

At high redshift, the ISW effect would be null on all scales for M_ν=0, while for M_ν>0 it is still active on small scales because of free-streaming.

CC et al. 2016

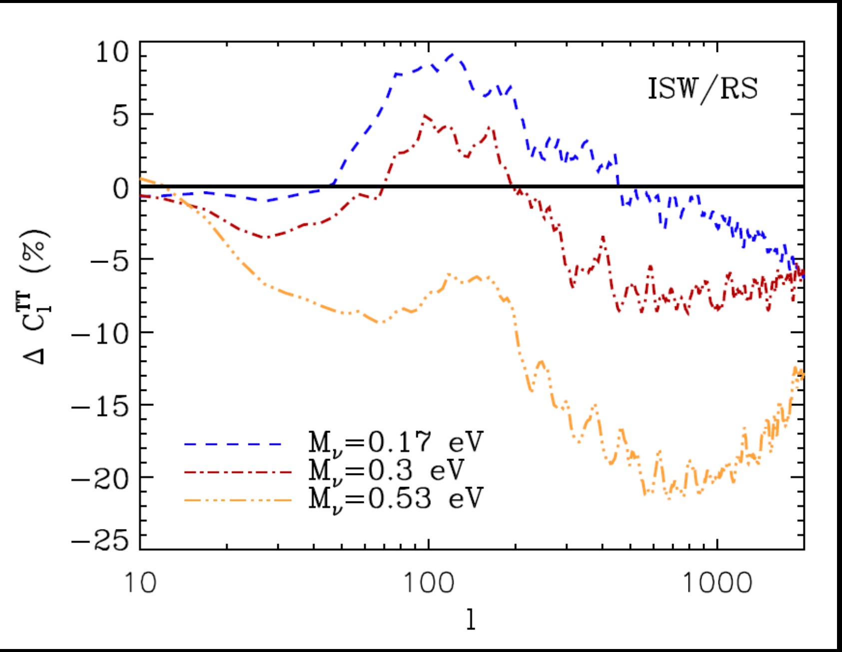

$$k_{\mathrm{fs}}(z) = 0.82H(z)/H_0/(1+z)^2(m_\nu/1\mathrm{eV}) \;\; h\,\mathrm{Mpc}^{-1}$$

ISWRS-CMBlens cross correlation

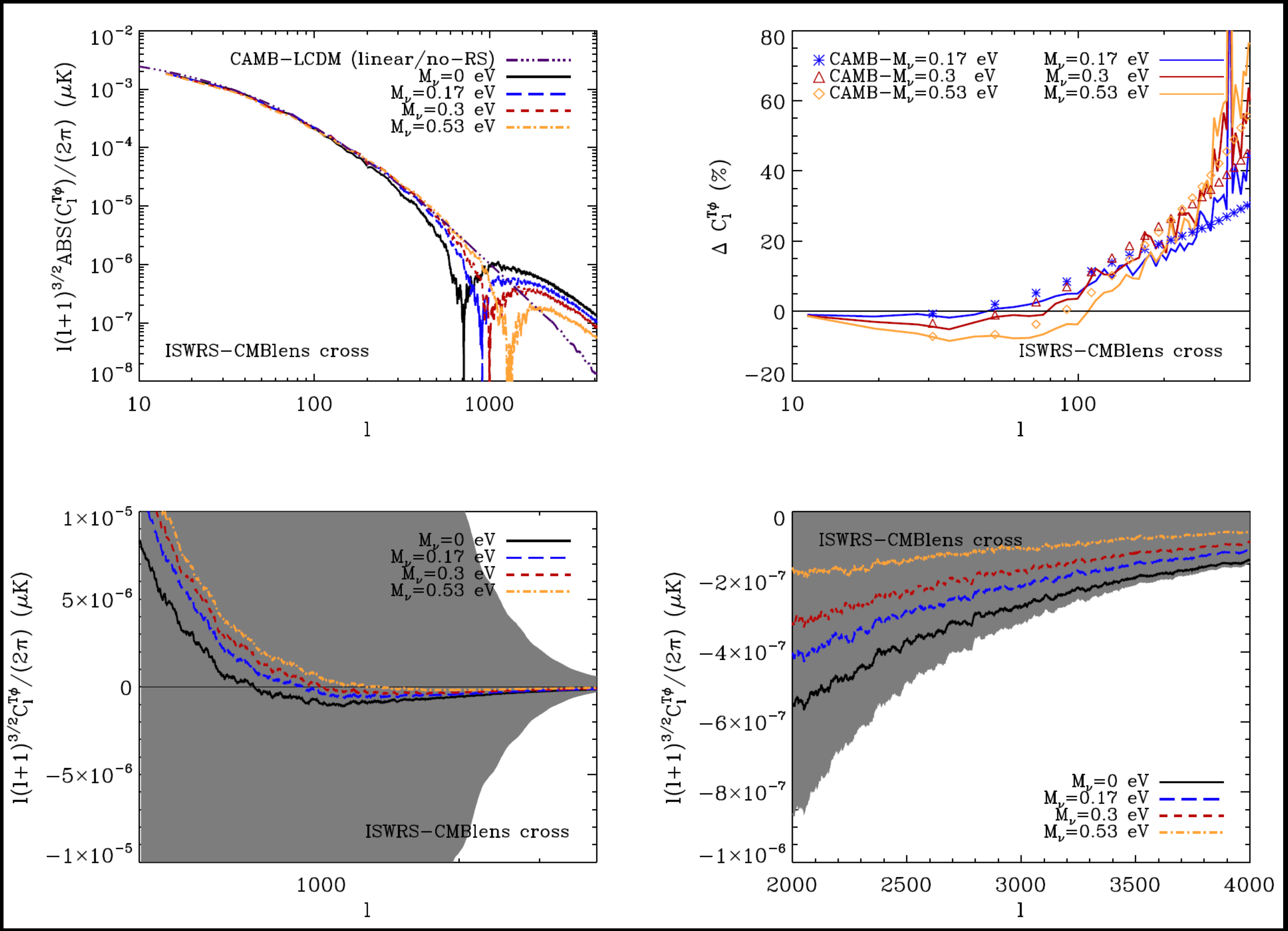

CC et al. 2016

Sign inversion: the non-linear transition moves toward smaller scales with increasing neutrino mass

ISWRS-Weaklens cross correlation

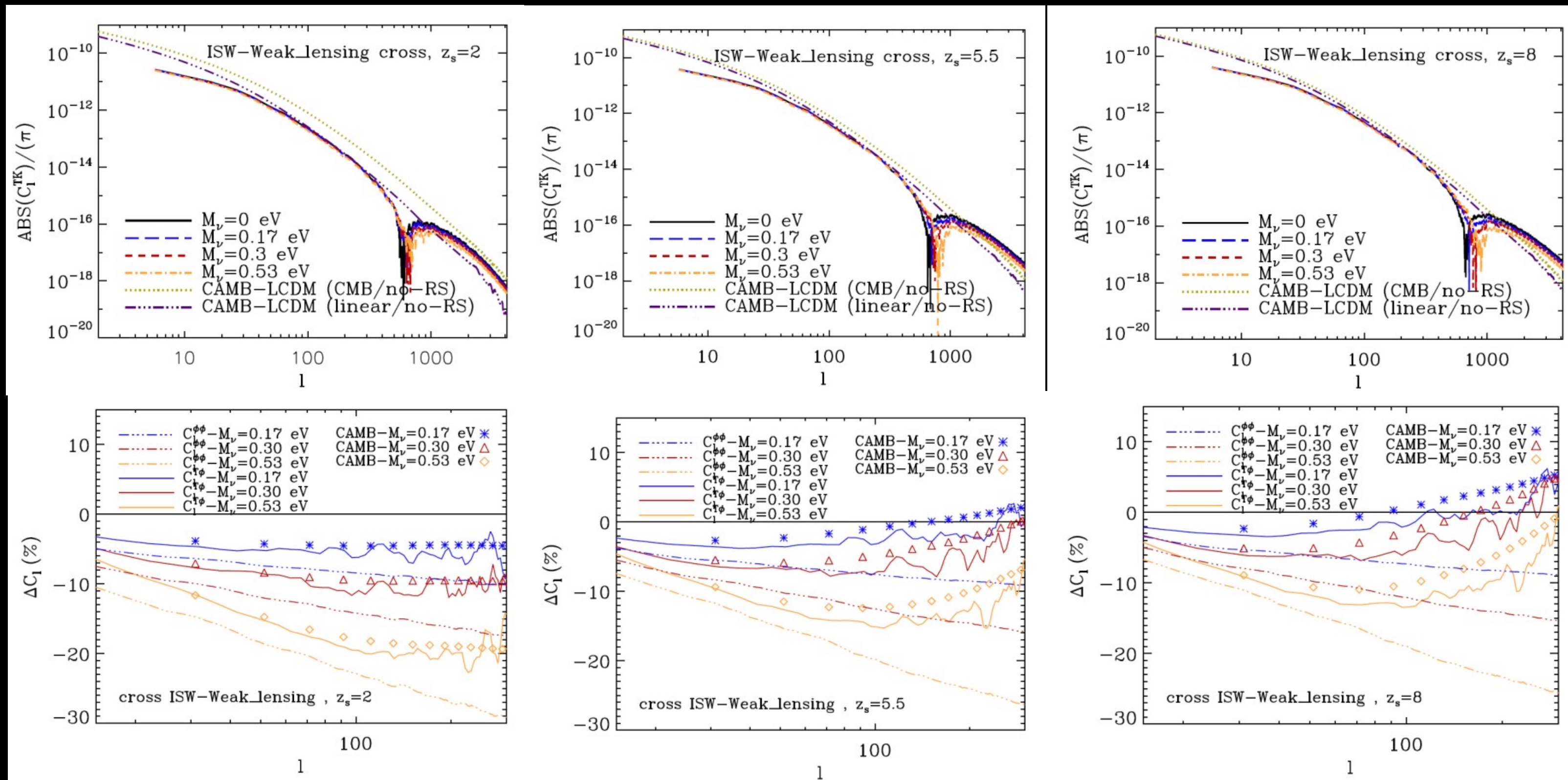

CC et al. 2016

Difference depends on the source redshift. Excess of power of the cross signal with respect to the auto-correlation signal.

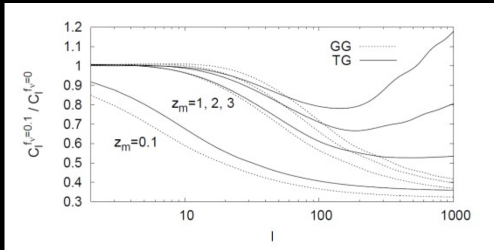

FIG. 2: Ratio of the cross-correlation multipoles C_l^{TG} and auto-correlation multipoles C_l^{GG} obtained for two cosmological models with neutrino density fractions equal to $f_\nu = 0.1$ or 0, and the same value of other cosmological parameters (see the text for details).

(Lesgourgues et al. 2008)

ISW-galaxy correlation predictions as function of the median redshift

DEMNUni collaboration

- Initial conditions: M. Zennaro, J. Bel, F. Villaescusa, C. Carbone, E. Sefusatti
- P-Gadget3 code with massive neutrinos: M. Viel, V. Springel, K. Dolag, M. Petkova
- Simulation runs: C. Carbone
- CMB-lensing and ISW/Rees-Sciama: C. Carbone
- Galaxy clustering: E. Castorina, M. Zennaro, J. Bel, C. Carbone, E. Sefusatti
- HOD/SAM with massive neutrinos: M. Zennaro, R. Angulo, A. J. Hawken
- SZ-maps and cross-correlation with lensing: M. Roncarelli, M. Calabrese, C. Carbone
- Cross-correlation clusters/weak-lensing: M. Calabrese, C. Carbone
- High-order statistics: R. Ruggeri, E. Castorina, J. Bel, E.Sefusatti
- Voids with massive neutrinos: A. J. Hawken, B. Granett

Conclusions

- ✓ **Very large neutrino simulations for different probe combinations**
- ✓ **Previous results on bias and MF recovered and confirmed**
- ✓ **New Halofit prescription to account for massive neutrinos**
- ✓ **Good behaviour of exiting PT approximations if applied to CDM alone.**
- ✓ **Detection of the scale dependent growth-rate at linear scales**
- ✓ **Suppression of the CMB/weak-lensing signals, depending on the neutrino mass and source redshifts**
- ✓ **Enhancement of power at the ISW-RS transition of about 10% due to neutrino free-streaming**
- ✓ **Enhancement of the ϕT cross-correlation in the case of the CMB lensing-potential, and for high redshift lensed sources, depending on the neutrino mass**
- ✓ **Suppression of ϕT cross-correlation for low median redshift surveys, but anyway larger than $\phi\,\phi$ auto-correlation.**